6. Fujii, N.; Nakai, K.; Tamamura, H.; Otaka, A.; Mimura, N.; Miwa, Y.; Taga, T.; Yamamoto, Y.; Ibuka, T. *J. Chem. Soc., Perkin Trans. 1* **1995**, 1359–1371.
7. Ohtani, I.; Kusumi, T.; Kashman, Y.; Kakisawa, H. *J. Am. Chem. Soc.* **1991**, *113*, 4092–4096.
8. McKinney, J. A.; Eppley, D. F.; Keenan, R. M. *Tetrahedron Lett.* **1994**, *35*, 5985–5988.
9. Yajima, H.; Fujii, N.; Funakoshi, S.; Watanabe, T.; Murayama, E.; Otaka, A. *Tetrahedron* **1988**, *44*, 805–819.
10. (a) Wakamiya, T.; Tarumi, Y.; Shiba, T. *Bull. Chem. Soc. Jpn.* **1974**, *47*, 2686–2689; (b) Tamamura, H.; Hori, T.; Otaka, A.; Fujii, N. *J. Chem. Soc., Perkin Trans. 1* **2002**, 577–580; (c) Sohma, Y.; Sasaki, M.; Hayashi, Y.; Kimura, T.; Kiso, Y. *Chem. Commun.* **2004**, 124–125.

Structure−Activity Relationships of Cyclic Peptide-Based Chemokine Receptor CXCR4 Antagonists: Disclosing the Importance of Side-Chain and Backbone Functionalities

Satoshi Ueda,[†] Shinya Oishi,[†] Zi-xuan Wang,[‡] Takanobu Araki,[†] Hirokazu Tamamura,[†,#] Jérôme Cluzeau,[†] Hiroaki Ohno,[†] Shuichi Kusano,[∥] Hideki Nakashima,[∥] John O. Trent,[§] Stephen C. Peiper,[‡] and Nobutaka Fujii[†,*]

Graduate School of Pharmaceutical Sciences, Kyoto University, Sakyo-ku, Kyoto 606-8501, Japan, Department of Pathology, Medical College of Georgia, Georgia 30912, Institute of Biomaterials and Bioengineering, Tokyo Medical and Dental University, Chiyoda-ku Tokyo 101-0062, Japan, St. Marianna University, School of Medicine, Miyamae-ku, Kawasaki 216-8511, Japan, and James Graham Brown Cancer Center, University of Louisville, Kentucky 40202

Received June 19, 2006

Previously, we have identified a highly potent CXCR4 antagonist **2** [cyclo(-D-Tyr[1]-Arg[2]-Arg[3]-Nal[4]-Gly[5]-)] and its Arg[2] epimer **3** [cyclo(-D-Tyr[1]-D-Arg[2]-Arg[3]-Nal[4]-Gly[5]-)] by the screening of cyclic pentapeptide libraries that were designed based on the structure−activity relationship studies on 14-residue peptidic CXCR4 antagonist **1**. In the present study, a new series of analogues of **2** and **3** were synthesized to evaluate the influences of peptide side-chain and backbone modification on bioactivities. Based on the Ala-scanning study, in which each residue in **2** and **3** was replaced with Ala having the identical chirality, substitution of Arg[3] and Nal[4] [Nal = L-3-(2-naphthyl)alanine] with Ala (compounds **6**, **7**, **10**, **11**) led to significant loss of the potency, indicating these amino acids are more important contributors to the bioactivity. For the cyclic peptide backbone, several modifications including D/L-Ala or cyclic amino acids substitution at the Gly[5] position and sequential *N*-methylation on amide nitrogens were conducted. Among the analogues, compounds **13** [cyclo(-D-Tyr[1]-Arg[2]-Arg[3]-Nal[4]-D-Ala[5]-)] and **32** [cyclo(-D-Tyr[1]-D-MeArg[2]-Arg[3]-Nal[4]-Gly[5]-)] were close in potency to the most potent lead **2**. NMR and conformational analysis indicated that both of these analogues favor the same backbone conformation as **2**, whereas similar analysis of less potent analogues indicates that an altered backbone conformation is favored. The conformational analysis showed that steric repulsion by a 1,3-allylic strain-like effect across the planar peptide bond might contribute to the conformational preferences of cyclic pentapeptides.

Introduction

Chemokines comprise a protein family of chemotactic factors that bind G protein-coupled receptors.[1,2] Engagement of chemokine receptors by their ligands triggers changes of the receptor conformation that lead to the initiation of a signaling cascade involving G protein binding, protein kinase activation, Ca^{2+} mobilization from intracellular stores, and cytoskeletal rearrangement, eventually leading to directed cell migration toward the gradients of the respective ligand.[3,4] A chemokine receptor CXCR4 and its endogenous ligand CXCL12 (stromal cell derived factor-1, SDF-1) are partners in multiple important functions in normal physiology involving the leukocyte chemotaxis in the immune system[5] and progenitor cell migration during embryologic development of the cardiovascular,[6,7] hemopoietic,[8] and central nervous systems.[9,10] On the other hand, CXCR4 has also multiple functions in pathologic physiology. CXCR4 serves as a coreceptor for infection of T cell line-tropic (X4) strains of the human immunodeficiency virus type 1 (HIV-1[a]). Following activation of the gp120 subunits of the envelope glycoprotein by binding to CD4, CXCR4 leads to membrane fusion and subsequent entry of the viral genome into the target cell.[11,12] Recently, Müller et al. disclosed that CXCL12/CXCR4 interactions participate in breast cancer metastasis analogous to programming directed migration in normal leukocytes and progenitor cells.[13] Expression of CXCR4 is enriched on the surface of malignant primary breast cancer cells while CXCL12 is preferentially expressed in organs that are frequent sites of metastasis in breast cancer, such as lung, liver, lymph nodes, and bone marrow. The coordinate actions between an attractant molecule and the corresponding receptor allow tumor cells to spread specifically to distant organs that provide a supportive niche. Furthermore, Nanki et al. reported that CXCL12/CXCR4 interactions might play a central role in memory T cell migration into inflamed rheumatoid arthritis (RA) synovium and for persisting inflammation at the affected site mediated by $CD4^+$ T cells.[14]

Thus, CXCR4 is considered as an important therapeutic target for multiple diseases. Several potent CXCR4 antagonists have been developed so far. Among them, a β-sheet-like 14-residue peptide **1** was identified by potency optimization of a 18-residue cyclic peptide isolated from horseshoe crabs (Figure 1).[15] The peptide **1** and its analogues were also characterized as HIV-1 entry inhibitors,[16] anticancer-metastatic,[17,18] and anti-RA agents.[19] Several other low-molecular-weight CXCR4 antagonists such as AMD3100[20,21] and KRH1636[22] have also been reported to inhibit HIV-1 infection through CXCR4. Recently, we have identified novel potent CXCR4 antagonists **2** and **3** by screening of two orthogonal cyclic pentapeptide libraries,[23] which were designed based on the structure−activity relationship studies on **1** (Figure 1).[24] These peptides contain two arginine, one 3-(2-naphthyl)alanine, and one tyrosine residue, that potentially

* Corresponding author. Tel: +81-75-753-4551, Fax: +81-75-753-4570, E-mail: nfujii@pharm.kyoto-u.ac.jp
† Kyoto University.
‡ Medical College of Georgia.
# Tokyo Medical and Dental University.
∥ St. Marianna University.
§ University of Louisville.

[a] Abbreviations: Nal, L-3-(2-naphthyl)alanine; Pic, pipecolic acid; Sar, sarcosine; HIV-1, human immunodeficiency virus type 1; RA, rheumatoid arthritis; SA-MD, simulated annealing molecular dynamics; AMD3100, 1,1′-[1,4-phenylenebis(methylene)]-bis(1,4,8,11-tetraazacyclotetradecane); KRH1636, *N*-{(*S*)-4-guanidino-1-[(*S*)-1-naphthalen-1-yl-ethylcarbamoyl]butyl}-4-{[(pyridin-2-yl-methyl)amino]methyl}benzamide.

10.1021/jm0607350 CCC: $37.00
Published on Web 12/29/2006

Scheme 1[a]

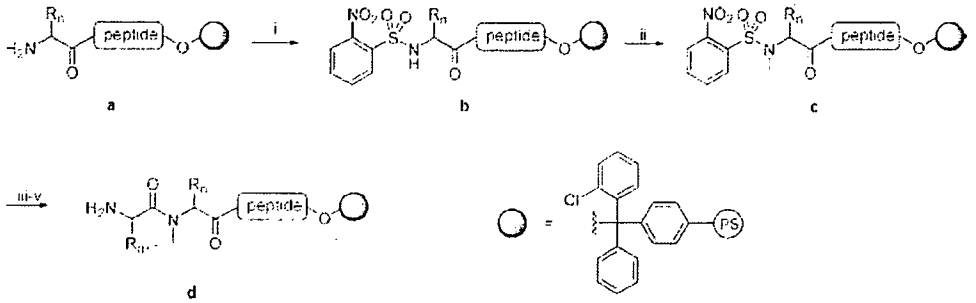

[a] Reagents: (i) *o*-nitrobenzenesulfonyl chloride, 2,4,6-collidine; (ii) MeOH, PPh_3, DEAD; (iii) DBU, 2-mercaptoethanol; (iv) Fmoc-AA-OH, HATU, HOAT, DIPEA; (v) piperidine.

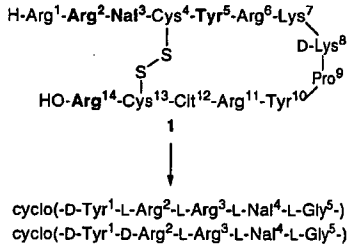

2 cyclo(-D-Tyr[1]-L-Arg[2]-L-Arg[3]-L-Nal[4]-L-Gly[5]-)
3 cyclo(-D-Tyr[1]-D-Arg[2]-L-Arg[3]-L-Nal[4]-L-Gly[5]-)

Figure 1. Structures of **1** and its downsized peptides **2** and **3**. Bold residues are the indispensable residues of **1** for the potent CXCR4-antagonistic activity. Nal = L-3-(2-naphthyl)alanine, Cit = L-citrulline.

correspond to the pharmacophore residues of the parent peptide **1**. We[25-27] and others[28] have performed several modifications on **2** including incorporation of (*E*)-alkene or reduced-amide dipeptide isosteres and conformationally constrained amino acid analogues, and fine-tuning of backbone ring structures. However, systematic modifications of **2** to design more potent antagonists have not been reported so far. In order to clarify the elements among the peptide side-chain and backbone functional groups indispensable for the ligand binding to CXCR4, chemical derivatization of **2** and **3** was conducted. In this manuscript, we describe the details of structure−activity relationship studies on cyclic pentapeptide-based CXCR4 antagonists **2** and **3** as well as identification of a more potent CXCR4 antagonist.

Chemistry. Synthesis on solid support of all peptides was performed on 2-chlorotrityl [(2-Cl)Trt] resin in parallel using usual Fmoc-based solid-phase peptide synthesis as described in the Experimental Section. *t*-Bu and 2,2,4,6,7-pentamethyldihydrobenzofuran-5-sulfonyl (Pbf) groups were employed for Tyr and Arg residue side-chain protection, respectively. L-Ala, D-Ala, L-Pro, D-Pro, L-pipecolic acid (L-Pic), D-Pic, β-alanine (β-Ala), and L-Nal were employed for the C-terminal residues of **12/19**, **13/20**, **14/21**, **15/22**, **16/23**, **17/24**, **18/25**, and **26/31**, respectively. The Gly residue was positioned at the C-terminal of the other peptide resins to avoid potential epimerization during the cyclization. For the preparation of *N*-methyl amino acid-containing peptide resins, an *N*-methyl group was incorporated on the α-amino group by a site-selective method reported by Miller et al.[29,30] (Scheme 1). The α-amino group was temporarily protected with an *o*-nitrobenzenesulfonyl (*o*-Ns) group before *N*-methylation by the Mitsunobu reaction. After removal of the *o*-Ns group by treatment with 1,8-diazabicyclo[5.4.0]undec-7-ene (DBU) and 2-mercaptoethanol, the subsequent amino acids were coupled using *O*-(7-azabenzotriazol-1-yl)-1,1,3,3-tetramethyluronium hexafluorophosphate (HATU)[31] as an activating reagent. Treatment of protected peptide resins with 20% (v/v) 1,1,1,3,3,3-hexafluoroisopropanol (HFIP) in CH_2Cl_2[32] provided linear protected peptides, which were cyclized with diphenylphosphoryl azide (DPPA) in DMF. Final deprotection with TFA−H_2O (95:5) followed by reverse-phase HPLC purification afforded the cyclic peptides. All peptides were identified with ion-spray mass spectrometry, and the purity was more than 95% by analytical HPLC.

Table 1. Biological Activities of **2**, **3**, and the Ala-Substituted Derivatives

peptide	sequence[a]	IC_{50} (μM)[b]	EC_{50} (μM)[c]
2	cyclo(-D-Tyr-L-Arg-L-Arg-L-Nal-Gly-)	0.004	0.16
4	cyclo(-D-Ala-L-Arg-L-Arg-L-Nal-Gly-)	>1	115
5	cyclo(-D-Tyr-L-Ala-L-Arg-L-Nal-Gly-)	0.063	12
6	cyclo(-D-Tyr-L-Arg-L-Ala-L-Nal-Gly-)	>1	>120
7	cyclo(-D-Tyr-L-Arg-L-Arg-L-Ala-Gly-)	>1	>120
3	cyclo(-D-Tyr-D-Arg-L-Arg-L-Nal-Gly-)	0.008	0.39
8	cyclo(-D-Ala-D-Arg-L-Arg-L-Nal-Gly-)	0.13	29
9	cyclo(-D-Tyr-D-Ala-L-Arg-L-Nal-Gly-)	0.23	16
10	cyclo(-D-Tyr-D-Arg-L-Ala-L-Nal-Gly-)	>1	60
11	cyclo(-D-Tyr-D-Arg-L-Arg-L-Ala-Gly-)	>1	>120

[a] The substituted residues from the parent peptides **2** and **3** are designated by underlining. [b] IC_{50} values for the cyclic pentapeptides are based on inhibition of [^{125}I]SDF-1 binding to CXCR4 transfectants of CHO cells. [c] EC_{50} values are based on the inhibition of HIV-induced cytopathogenicity in MT-4 cells. All data are the mean values for at least three independent experiments.

Results and Discussion

Identification of Indispensable Pharmacophore Functionality by Alanine-Scanning. Our first attempt was to identify the minimal side-chain functional group requirement of **2** and **3** for CXCR4 antagonism. To evaluate the comparative significance of side-chain functionality, each residue except for the Gly residue of **2** and **3** was substituted with Ala. Because the chirality of Ala was identical to that of the corresponding residue in parent peptides, exhibition of similar conformations was expected even after the substitution. All Ala-substituted peptides **4**−**11** showed significantly less CXCR4 antagonistic and anti-HIV activities when compared to the parent peptides **2** and **3**. Ala[3]- or Ala[4]-substituted analogues **6**, **7**, **10**, and **11** did not show any CXCR4 antagonistic activity up to 1 μM (Table 1). This indicates that all the side-chain functional groups are important for the high CXCR4 antagonistic activity. On the other hand, L/D-Ala[2]-substituted analogues, **5** and **9**, and D-Ala[1]-substituted analogue **8** maintained moderate activities (**5**: IC_{50} = 63 nM, EC_{50} = 12 μM; **8**: IC_{50} = 130 nM, EC_{50} = 29 μM; **9**: IC_{50} = 230 nM, EC_{50} = 16 μM), although the potencies were less than one-twentieth of the parent peptides. These data suggest that the phenol group of D-Tyr[1] and a guanidino group of Arg[2] do not play a critical role in receptor binding, while guanidino group of Arg[3] and naphthalene group of Nal[4] are indispensable for the ligand interaction with CXCR4. This

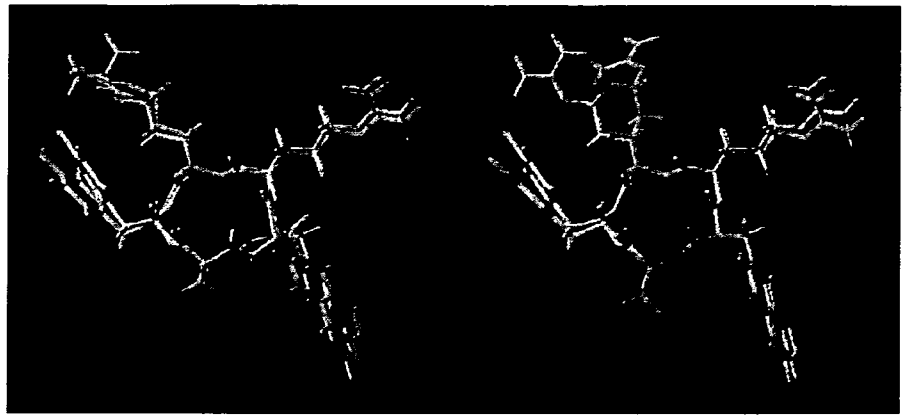

Figure 2. Superimposition of low-energy structures of **2** (purple) and **12** (green, left) or **13** (green, right).

propensity is consistent with the previous structure−activity relationship studies on **1**, where Ala-substitutions at the Arg^2-Nal^3 motif in **1** were more sensitive to anti-HIV activity as compared to the substitution of the other important residues, such as Tyr^5 and Arg^{14}.[24] It is noteworthy that two L/D-Ala^2-substituted peptides **5** and **9** having opposite chiralities retained moderate bioactivities. Recently, we have shown that L-Arg^2 in **2** could be replaced by nonbasic amino acids such as L-Phe-(4-F) (L-4-fluorophenylalanine) and D-MeAla without significant loss of CXCR4 antagonistic activity.[26,27] Hence, the functional group or the spatial disposition of the Arg^2 guanidino group could be further optimized.

Conformational Restriction of Cyclic Peptides by Modification of the Glycine Residue. In contrast to the finding that all side-chain functional groups of **2** and **3** were important for the high CXCR4 antagonistic activities, the Gly^5 position had many possibilities for further optimization. Since the absence of a side chain in Gly^5 possibly affected the conformational flexibility of the peptide backbone, it was expected that use of chiral or conformationally constrained amino acids would potentially restrict the global conformations to decrease the entropy losses upon the peptide binding on CXCR4. In order to evaluate the structure−activity relationship at the Gly^5 position, simple aliphatic amino acids were utilized for this study. In our previous conformational studies on **2**, characteristic orientations of the amide carbonyl groups of D-Tyr,^{1} Arg,^{2} Arg^3, and Gly^5 were observed in the low energy state.[23] These carbonyl oxygens were oriented away from the side chains of the respective following amino acids. This could be attributed to steric repulsion by a 1,3-allylic strain-like effect across the planar peptide bond.[33] On the other hand, the flexible Nal^4 ψ and Gly^5 ϕ angles had been expected, since there were two possibilities of Nal^4 carbonyl oxygen orientation. However, the carbonyl oxygen was directed away from the Gly^5 pro-*R* hydrogen atom in the calculated conformations, while the other orientation was not exhibited. This implied that the incorporation of a side chain having *R*-chirality (D-amino acid) at the Gly^5 position could restrict the rotation of the Nal^4-Gly^5 peptide bond plane. On the basis of this hypothesis, we introduced both enantiomers of Ala, Pro, and Pic to the Gly^5 position for conformational restriction. In addition, β-Ala was utilized for the optimization of carbon chain length at the Gly^5 position.

L-Ala^5-substituted analogues **12** and **19** showed less than 10-fold lower CXCR4 antagonistic and anti-HIV activities of the parent peptides **2** and **3**, respectively (Table 2, **12**: IC_{50} = 170 nM; EC_{50} = 20 μM, **19**: IC_{50} = 92 nM; EC_{50} = 10 μM). By contrast and as expected, more than 8-fold higher potencies were observed for D-Ala^5-substituted analogues **13** and **20** (**13**: IC_{50} = 11 nM; EC_{50} = 0.49 μM, **20**: IC_{50} = 11 nM; EC_{50} = 0.67 μM) as compared to the corresponding L-Ala^5-substituted peptides **12** and **19**, respectively. The bioactivities of D-Ala^5-substituted analogues were approximately half of the parent peptides **2** and **3**. This suggested that substitution with L-Ala^5 resulted in significant conformational change, while D-Ala^5 substitution kept the bioactive conformations of the parent peptides **2** and **3**. Simulated annealing molecular dynamics (SA-MD) analysis demonstrated that the backbone conformation of **13** was similar to that of **2** but different from that of **12** (Figure 2). Local conformations around Nal^4 and Gly^5/D-Ala^5 were very similar between **2** and **13** as expected, while the conformation of L-Ala^5-substituted analogues **12** differed particularly in the opposite orientation of the Nal^4 carbonyl oxygen. These calculated structures are consistent with the observed NOE data; in L-Ala^5-substituted peptide **13**, strong NOE between Nal^4 H$^\alpha$ and D-Ala^5 H^N indicates that these hydrogen atoms were oriented into the same direction. On the other hand, the observed weak NOE between Nal^4 H$^\alpha$ and L-Ala^5 H^N in peptide **12** indicates these hydrogen atoms were oriented into the opposite directions. The 1,3-pseudo allylic strain between the Nal^4 carbonyl oxygen and the α-methyl group of D/L-Ala^5 could result in these different conformational preferences between **12** and **13**. This

Table 2. Biological Activities of the Gly^5-Modified Analogues of **2** and **3**

peptide	sequence[a]	IC_{50} (μM)[b]	EC_{50} (μM)[c]
2	cyclo(-D-Tyr-L-Arg-L-Arg-L-Nal-Gly-)	0.004	0.16
12	cyclo(-D-Tyr-L-Arg-L-Arg-L-Nal-L-Ala-)	0.17	20
13	cyclo(-D-Tyr-L-Arg-L-Arg-L-Nal-D-Ala-)	0.011	0.49
14	cyclo(-D-Tyr-L-Arg-L-Arg-L-Nal-L-Pro-)	>1	-[d]
15	cyclo(-D-Tyr-L-Arg-L-Arg-L-Nal-D-Pro-)	>1	-[d]
16	cyclo(-D-Tyr-L-Arg-L-Arg-L-Nal-L-Pic-)	>1	-[d]
17	cyclo(-D-Tyr-L-Arg-L-Arg-L-Nal-D-Pic-)	>1	-[d]
18	cyclo(-D-Tyr-L-Arg-L-Arg-L-Nal-β-Ala-)	0.047	3.0
3	cyclo(-D-Tyr-D-Arg-L-Arg-L-Nal-Gly-)	0.008	0.37
19	cyclo(-D-Tyr-D-Arg-L-Arg-L-Nal-L-Ala-)	0.092	10
20	cyclo(-D-Tyr-D-Arg-L-Arg-L-Nal-D-Ala-)	0.011	0.67
21	cyclo(-D-Tyr-D-Arg-L-Arg-L-Nal-L-Pro-)	> 1	-[d]
22	cyclo(-D-Tyr-D-Arg-L-Arg-L-Nal-D-Pro-)	> 1	-[d]
23	cyclo(-D-Tyr-D-Arg-L-Arg-L-Nal-L-Pic-)	0.64	-[d]
24	cyclo(-D-Tyr-D-Arg-L-Arg-L-Nal-D-Pic-)	> 1	-[d]
25	cyclo(-D-Tyr-D-Arg-L-Arg-L-Nal-β-Ala-)	0.35	38

[a] The substituted residues from the parent peptide **2** and **3** are underlined. [b] IC_{50} values for the cyclic pentapeptides are based on inhibition of [^{125}I]SDF-1 binding to CXCR4 transfectants of CHO cells. [c] EC_{50} values are based on the inhibition of HIV-induced cytopathogenicity in MT-4 cells. [d] Not tested. All data are the mean values for at least three independent experiments.

Table 3. Biological Activities of *N*-Methyl Amino Acid-Containing Analogues of **2** and **3**

peptide	sequence[a]	IC_{50} (μM)[b]	EC_{50} (μM)[c]
2	cyclo(-D-Tyr-L-Arg-L-Arg-L-Nal-Gly-)	0.004	0.16
26	cyclo(-D-MeTyr-L-Arg-L-Arg-L-Nal-Gly-)	0.128	-[d]
27	cyclo(-D-Tyr-L-MeArg-L-Arg-L-Nal-Gly-)	0.023	1.399
28	cyclo(-D-Tyr-L-Arg-L-MeArg-L-Nal-Gly-)	0.099	9.534
29	cyclo(-D-Tyr-L-Arg-L-Arg-L-MeNal-Gly-)	0.250	-[d]
30	cyclo(-D-Tyr-L-Arg-L-Arg-L-Ala-Sar-)	0.167	-[d]
3	cyclo(-D-Tyr-D-Arg-L-Arg-L-Nal-Gly-)	0.008	0.39
31	cyclo(-D-MeTyr-D-Arg-L-Arg-L-Nal-Gly-)	0.157	-[d]
32	cyclo(-D-Tyr-D-MeArg-L-Arg-L-Nal-Gly-)	0.003	0.088
33	cyclo(-D-Tyr-D-Arg-L-MeArg-L-Nal-Gly-)	0.021	0.782
34	cyclo(-D-Tyr-D-Arg-L-Arg-L-MeNal-Gly-)	0.563	-[d]
35	cyclo(-D-Tyr-D-Arg-L-Arg-L-Nal-Sar-)	0.256	-[d]

[a] *N*-Methylated residues are underlined. [b] IC_{50} values for the cyclic pentapeptides are based on inhibition of [^{125}I]SDF-1 binding to CXCR4 transfectants of CHO cells. [c] EC_{50} values are based on the inhibition of HIV-induced cytopathogenicity in MT-4 cells. [d] Not tested. All data are the mean values for at least three independent experiments.

could explain the reason for the higher potencies of D-Ala[5]-substituted analogues. The above information could serve for the further optimization of the Gly[5] position using D-amino acids having side-chain functionality.

Our next approach was to restrict global conformations of peptides **2** and **3** using cyclic amino acids such as L/D-Pro and L/D-Pic. These amino acids can provide a fused ring structure of cyclic peptides consisting of small and large rings. It was expected that the limited ϕ angle flexibility of Pro and Pic could contribute to the global conformational restriction.[34] Covalent linkage between the amide nitrogen and the side chain could also produce a favorable orientation of the Nal[4] carbonyl oxygen. However, L/D-Pro[5]- and L/D-Pic[5]-substituted peptides **14**−**17**, **21**, **22**, and **24** did not show CXCR4 inhibitory activities with IC_{50} values lower than 1 μM. Even the most potent peptide **23** exhibited an IC_{50} of only 0.64 μM. This suggests that the presence of cyclic amino acids at this position is sterically or conformationally unfavorable for the peptide−CXCR4 interaction. We could also assume that an amide proton at this position is required for high activity. This was supported by the fact that peptides having a sarcosin (Sar) at the Gly[5] position possessed less than one-thirtieth CXCR4 antagonistic activity of the parent peptides (see the next section). β-Ala[5]-substituted analogues **18** and **25** showed lower CXCR4 antagonistic and anti-HIV activities (**18**: IC_{50} = 47 nM, EC_{50} = 3 μM; **25**: IC_{50} = 350 nM, EC_{50} = 38 μM), indicating that expansion of the backbone ring size (16-membered ring) at this position is not favorable. Recently, we showed that reduction in the size of the backbone ring using γ-Nal [4-amino-5-(2-naphthyl)pentanoic acid] or γ-(*E*)-Nal [(*E*)-4-amino-5-(2-naphthyl)pent-2-enoic acid] unit (14-membered ring) instead of Nal[4]-Gly[5] dipeptide resulted in moderate to significant loss of CXCR4 antagonistic activity.[27] These observations suggest the importance of Gly[5] as a spacer for appropriate spatial orientation of the CXCR4 antagonist pharmacophores.

Identification of a Novel Potent CXCR4 Antagonist through *N*-Methyl Amino Acid-Scanning of 2 and 3. *N*-Methylation of the peptide backbone has been shown to be a valuable method in structure−activity relationship studies on bioactive peptides.[35−37] Substitutions with *N*-methyl amino acids often cause an increase or decrease in potency and selectivity of peptide ligands, providing useful information on the bioactive conformation. Hence, every amide bond of **2** and **3** was replaced sequentially with the corresponding *N*-methylated amide, and the bioactivities of obtained peptides were evaluated (Table 3). Peptides **26**, **28**, **29**, and **30** derived from *N*-methyl amino acid-scanning of peptide **2** showed more than 25-fold less CXCR4 antagonistic activity as compared to the parent peptide **2**. *N*-Methylated analogues **31**, **34**, and **35** also showed a significant decrease in CXCR4 antagonism as compared to the parent peptide **3**. Use of L-MeArg[3] in peptide **33** slightly decreased the activity. *N*-Methylation at the Nal[4] position caused a remarkable decrease in CXCR4 antagonistic activity (**29**: IC_{50} = 250 nM; **34**: IC_{50} = 563 nM), suggesting that *N*-methylation at the putative receptor-binding motif (Arg[3]-Nal[4]) is unfavorable probably due to the absence of an amide proton. Previously, we showed that replacement of the Arg[3]-Nal[4] motif with the corresponding (*E*)-alkene dipeptide isostere unit (L-Arg[3]-ψ[(*E*)-CH=CH]-L-Nal[4]) or a reduced amide isostere unit (L-Arg[3]-ψ-[CH_2−NH]-L-Nal[4]) caused a significant loss of CXCR4 antagonistic activity.[25] These observations also indicate the importance of the Arg[3]-Nal[4] amide bond in both functional and conformational aspects.

On the other hand, the L/D-MeArg[2]-substituded peptides **27** and **32** showed potent CXCR4 antagonistic and anti-HIV activities (**27**: IC_{50} = 23 nM, EC_{50} = 1.4 μM; **32**: IC_{50} = 3.0 nM, EC_{50} = 0.088 μM), indicating that *N*-methylation at Arg[2] is not critical to antagonist activity. Interestingly, the D-MeArg[2] substitution (**32**) led to approximately 2-fold increase of CXCR4 antagonistic activity and more than 40-fold anti-HIV activity as compared with **3**, and these activities were nearly equal to those of **2**. NMR and SA-MD calculations showed that major conformer of **32** exhibited a backbone conformation similar to **2** but different from the parent peptide **3**, particularly with respect to the orientation of D-Tyr[1] carbonyl oxygen (Figure 3).[38] This conformation was also supported by strong NOEs between [D-Arg[2] H^{α} and D-Arg[2] H^{NMe}] and [D-Arg[2] H^{NMe} and Arg[3] H^{N}] in **32** (the corresponding strong NOEs were not observed in the parent peptide **3**; see Supporting Information). It is possible that an unfavorable 1,3-pseudo-allylic strain-like effect between the *N*-methyl group of D-MeArg[2] and D-Tyr[1] side chain of **32** induced the flip of D-Tyr[1]-D-Arg[2] amide group upon *N*-methylation of D-Arg[2], resulting in the identical local conformation around the D-Tyr[1]-D-MeArg[2] dipeptide with the D-Tyr[1]-L-Arg[2] conformation of **2**. Previously, we have shown a similar local conformational change upon *N*-methylation at the same position in D-Ala[2]-substituted analogues of **2**; i.e. cyclo(-D-Tyr[1]-D-MeAla[2]-Arg[3]-Nal[4]-Gly[5]-) showed 5-fold higher CXCR4 antagonistic activity (IC_{50} = 42 nM) than the nonmethylated peptide, cyclo(-D-Tyr[1]-D-Ala[2]-Arg[3]-Nal[4]-Gly[5]-) **9**.[27] It is also noted that the lower bioactivities of peptide **27** compared to **2** could be explained by the potential flip of the D-Tyr[1]-L-MeArg[2] amide bond orientation by *N*-methylation. These data suggest that the amide proton of Arg[2] has little contribution to bioactivity, and the amide bond orientation between D-Tyr[1] and D-MeArg[2] in **32** may contribute to its enhanced biological function.

Conclusion

Our present Ala-scanning study has shown that all of the side-chain functional groups contribute to high CXCR4 antagonistic activity of peptides **2** and **3**. In particular, Arg[3] and Nal[4] were proven to be indispensable for CXCR4 antagonistic activity. We have also shown that L-Ala substitution for Gly[5] of **2** or **3** caused a remarkable decrease in CXCR4 antagonistic and anti-HIV activities, while D-Ala substitution retained activity. Conformational studies revealed that D-Ala-substituted analogue **13** adopted a backbone conformation similar to that of **2**, which allows the rationalization of the biological activity for these

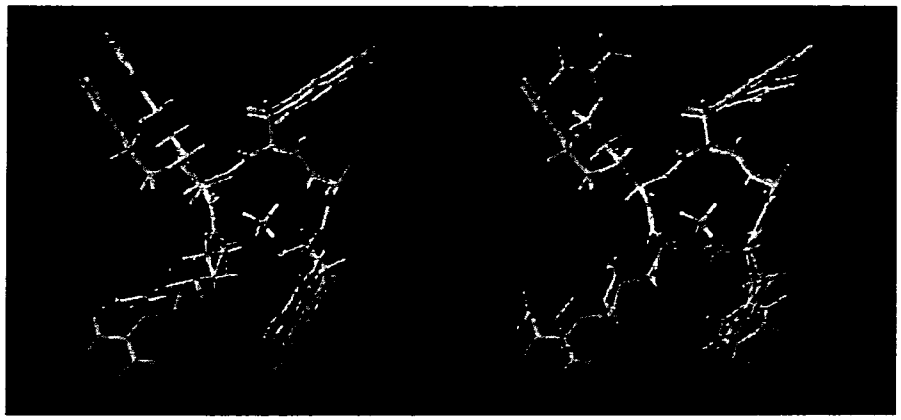

Figure 3. Superimposition of low-energy structures of **32** (green) and **2** (purple, left) or **3** (purple, right).

series of analogues. In addition, through comprehensive *N*-methyl-scanning of all residues in **2** and **3**, the *N*-methylated analogue **32** was characterized as one of the most potent cyclic pentapeptide-based CXCR4 antagonists synthesized thus far. The slight increase in CXCR4 antagonistic activity in **32** as compared to its nonmethylated analogue **3** could be explained by the favorable peptide bond orientation at the *N*-methylation site. Conformational studies suggested that the high potency in these series of compounds is due to the orientation of the backbone amide bonds, although direct interaction of the amide functions with the CXCR4 receptor is not clear. These results give valuable insight for understanding the ligand–receptor interactions and may also provide useful approaches for the design of new low-molecular-weight CXCR4 antagonists.

Experimental Section

General. Exact mass (HRMS) spectra were recorded on a JEOL JMS-01SG-2 or JMS-HX/HX 110A mass spectrometer. The ion-spray mass spectrum was obtained with a Sciex API*II*/*IE* triple quadrupole mass spectrometer (Toronto, Canada). Optical rotations were measured in water or 50% (v/v) water/AcOH solution with a Horiba high-sensitive polarimeter SEPA-200. ^{1}H NMR spectra were recorded using a Bruker AM 600 or JEOL JNM-ECA600 spectrometer at 600 MHz frequency, or JEOL JNM-AL400 spectrometer at 400 MHz frequency. Chemical shifts are calibrated to the solvent signal (2.49 ppm for DMSO, or 4.65 ppm for H_2O; s = singlet, d = doublet, dd = double doublet, m = multiplet). For HPLC separations, a Cosmosil 5C18-ARII analytical column (Nacalai Tesque, 4.6 × 250 mm, flow rate 1 mL/min) or a Cosmosil 5C18-ARII preparative column (Nacalai Tesque, 20 × 250 mm, flow rate 11 mL/min) was employed, and eluting products were detected by UV at 220 nm. A solvent system consisting of 0.1% TFA in water (v/v, solvent A) and 0.1% TFA in MeCN (v/v, solvent B) was used for HPLC elution.

Preparation of Amino Acid-Loaded 2-Chlorotrityl Resin. 2-Chlorotrityl chloride resin (1.25 mmol/g, 0.63 mmol) was treated with Fmoc-amino acid (0.69 mmol) and *N*,*N*-diisopropylethylamine (DIPEA) (2.77 mmol) in CH_2Cl_2 (5.00 mL) for 1.5 h. After the resin was washed with CH_2Cl_2, it was dried in vacuo. The loading was determined by measuring at 290 nm UV absorption of the piperidine-treated sample: Fmoc-L-Nal-(2-Cl)Trt-resin (0.72 mmol/g); Fmoc-L-Pro-(2-Cl)Trt-resin (0.78 mmol/g); Fmoc-D-Pro-(2-Cl)-Trt-resin (0.81 mmol/g); Fmoc-L-Pic-(2-Cl)Trt-resin (0.88 mmol/g); Fmoc-D-Pic-(2-Cl)Trt-resin (0.84 mmol/g); Fmoc-β-Ala-(2-Cl)Trt-resin (0.79 mmol/g).

Fmoc-Based Solid-Phase Peptide Synthesis. Protected peptide resins were manually constructed on a 0.10 mmol scale on H-L-Ala-(2-Cl)Trt-resin (0.89 mmol/g) for **12** and **19**, H-D-Ala-(2-Cl)-Trt-resin (0.90 mmol/g) for **13** and **20**, Fmoc-L-Pro-(2-Cl)Trt-resin for **14** and **21**, Fmoc-D-Pro-(2-Cl)Trt-resin for **15** and **22**, Fmoc-L-Pic-(2-Cl)Trt-resin for **16** and **23**, Fmoc-D-Pic-(2-Cl)Trt-resin for **17** and **24**, Fmoc-β-Ala-(2-Cl)Trt-resin for **18** and **25**, Fmoc-L-Nal-(2-Cl)Trt-resin for **26** and **31**, and H-Gly-Trt(2-Cl)Trt-resin (0.75 mmol/g) for the other peptides. Fmoc-amino acids were coupled using 1,3-diisopropylcarbodiimide (DIPCDI, 0.078 mL, 0.50 mmol) and *N*-hydroxybenzotriazole hydrate (HOBt·H_2O, 76 mg, 0.50 mmol) in DMF (1.0 mL) for 1.5 h. For the coupling of Fmoc-amino acid to the *N*-methyl amino acid, HATU (186 mg, 0.49 mmol) and 1-hydroxy-7-azabenzotriazole (HOAt, 68 mg, 0.50 mmol) were employed in place of DIPCDI/HOBt. The Fmoc group was deprotected by treatment with 20% (v/v) piperidine–DMF for 20 min.

***N*-Methyl Modification of *N*-Terminal α-Amino Group on Resin.** Resin (0.10 mmol) was treated with *o*-nitrobenzenesulfonyl chloride (66.5 mg, 0.30 mmol) and 2,4,6-collidine (0.066 mL, 0.50 mmol) in CH_2Cl_2 (1.0 mL) for 2 h at room temperature. After the resin was washed (CH_2Cl_2 × 3, DMF × 3, and THF × 3), to a suspension of the *N*-Ns-protected resin in anhydrous THF (1.0 mL) were added MeOH (0.020 mL, 0.50 mmol), PPh_3 (131 mg, 0.50 mmol), and diethyl diazodicarboxylate (0.227 mL, 0.50 mmol) at 0 °C. The mixture was shaken for 2 h at room temperature, followed by washing the resin (THF × 3 and $CHCl_3$ × 3). The *N*-methylated resin was treated with DBU (0.075 mL, 0.50 mmol) and 2-mercaptoethanol (0.070 mL, 1.0 mmol) for 1.5 h at room temperature to give the protected peptide resin having an *N*-methyl amino acid at the *N*-terminus.

Cleavage of Protected Peptides from the Resin and Cyclization. Protected peptide resin was treated with 20% (v/v) HFIP–CH_2Cl_2 (10 mL) for 2 h. After filtration of the resin, the filtrate was concentrated to provide the crude linear protected peptide. To the solution of the residue in DMF (30 mL) were added DPPA (0.539 mL, 0.25 mmol) and $NaHCO_3$ (42.0 mg, 0.50 mmol) at −40 °C. After being stirred for 36 h at room temperature, the whole was filtered, and the filtrate was concentrated to give the protected cyclic peptide, which was subjected to solid-phase extraction (SPE) over basic alumina in $CHCl_3$–MeOH (9:1) to remove inorganic salts derived from DPPA.

Deprotection of Protected Cyclic Peptide and HPLC purification. Protected cyclic peptides were treated with 95% (v/v) TFA solution (10 mL) for 2 h at room temperature. Concentration under reduced pressure and purification by preparative HPLC gave cyclic peptides.

Cell Culture. Human T-cell lines, MT-4 and MOLT-4 cells were grown in RPMI 1640 medium containing 10% heat-inactivated fetal calf serum, 100 IU/mL penicillin, and 100 μg/ mL streptomycin.

Virus. A strain of X4-HIV-1, HIV-1IIIB, was used for the anti-HIV assay. This virus was obtained from the culture supernatant of HIV-1 persistently infected MOLT-4/HIV1IIB cells and stored at −80 °C until used.

Anti-HIV-1 Assay. Anti-HIV-1 activity was determined based on the protection against HIV-1-induced cytopathogenicity in MT-4

cells. Various concentrations of test compounds were added to HIV-1 infected MT-4 cells at multiplicity of infection (MOI) of 0.01 and placed in wells of a flat-bottomed microtiter tray (1.5×10^4 cells/ well). After 5 days incubation at 37 °C in a CO_2 incubator, the number of viable cells was determined using the 3-(4,5-dimethylthiazol-2-yl)-2,5-diphenyltetrazolium bromide (MTT).

[^{125}I]-SDF-1 Binding and Displacement. Stable CHO cell transfectants expressing CXCR4 variant were prepared as describe previously.[39] CHO transfectants were harvested by treatment with trypsin−EDTA, allowed to recover in complete growth medium (MEM-α, 100 μg/ mL penicillin, 100 μg/mL streptomycin, 0.25 μg/mL amphotericin B, 10% (v/v)) for 4−5 h, and then washed in cold binding buffer (PBS containing 2 mg/mL BSA). For ligand binding, the cells were resuspended in binding buffer at 1×10^7 cell/mL, and 100 μL aliquots were incubated with 0.1 nM of [^{125}I]-SDF-1 (Perkin-Elmer Life Sciences) for 2 h on ice under constant agitation. Free and bound radioactivities were separated by centrifugation of the cells through an oil cushion, and bound radioactivity was measured with gamma-counter (Cobra, Packard, Downers Grove, IL). Inhibitory activity of test compounds was determined based on the inhibition of [^{125}I]-SDF-1 binding to CXCR4 transfectants (IC_{50}).

NMR Spectroscopy. The peptide sample was dissolved in DMSO-d_6 at a concentration of 5 mM. ^{1}H NMR spectra of the peptides were recorded at 300 K. The assignment of the proton resonance was achieved by use of ^{1}H−^{1}H COSY spectra. $^3J(H^N, H^\alpha)$ coupling constants were measured from one-dimensional spectra. The mixing time for NOESY experiments was set at 200 ms. NOESY spectra were composed of 512 real points in the F2 dimension and 256 real points, which were zero-filled to 256 points in the F1 dimension, with 144 scans per t1 increment. The cross-peak intensities were evaluated by relative build-up rates of the cross-peaks. **2**, **3**, **12**, and **13** exhibited one set of signals in ^{1}H NMR spectra. On the other hand, two distinct sets of signals were observed in ^{1}H NMR spectra of **32** with relative populations of 69% and 31%, indicating the existence of two conformations. For the minor conformer, NOESY spectra showed the NOE contact between α protons of D-Tyr^1 and D-MeArg^2 which is characteristic of the amide bond in a *cis* conformation. The major conformer did not exhibit any sequential H^α−H^α NOEs, suggesting this conformer adopt an all-*trans* conformation. The calculated structures of major and minor conformers exhibited *trans*- and *cis*-D-Tyr^1-D-MeArg^2 amide bond, respectively, which was consistent with the observed NOEs.

Calculation of Structures. The structure calculations were performed on a Silicon Graphics Origin 2000 workstation with the NMR refine program within the Insight II/Discover package using the consistent valence force field (CVFF). Pseudoatoms were defined for the CH_3^α protons of L-Ala^5 of **12**, D-Ala^5 of **13**, and *N*-methyl protons of **32**, and for all methylene protons of Nal^4, D-Tyr^1, D/L-Arg^2, and Arg^3, prochirality of which were not identified from ^{1}H NMR data. The dihedral ϕ angle constraints were calculated based on the Karplus equation: $^3J(H^N, H^\alpha) = 6.7\cos^2(\theta - 60°) - 1.3\cos(\theta - 60°) + 1.5$. Lower and upper angle errors were set to 15°. The NOESY spectrum with a mixing time of 200 ms was used for the estimation of the distances restraints between protons. The NOE intensities were classified into three categories (strong, medium, and weak) based on the number of contour lines in the cross-peaks to define the upper-limit distance restraints (1.7, 3.5, and 5.0 Å, respectively). The upper-limit restraints were increased by 1.0 Å for the involved pseudoatoms. Lower bounds between nonbonded atoms were set to their van der Waals radii (1.8 Å). These distance and dihedral angle restraints were included with force constants of 25−100 kcal/mol·Å^2 and 25−100 kcal/mol·rad^2, respectively. The 50 initial structures generated by the NMR refine program randomly were subjected to the simulated annealing calculations. The final minimization stage was achieved until the maximum derivative became less than 0.01 kcal/mol·Å^2 by the steepest descents and conjugate gradients methods. Excellent convergence was seen in the backbone structure of all calculated structures. The root-mean-square deviation (rmsd) values for all backbone structures of ten low-energy structures were below 0.23 Å.

Acknowledgment. This work was supported by Grant-in-Aid for Scientific Research from the Ministry of Education, Culture, Sports, Science, and Technology of Japan, and Health and Labour Sciences Research Grants (Research on HIV/AIDS) and Philip Morris USA Inc. and Philip Morris International. Computation time was provided by the Supercomputer Laboratory, Institute for Chemical Research, Kyoto University. S.U. and S.O. are grateful for the JSPS Research Fellowships for Young Scientists.

Supporting Information Available: Characterization data for all new compounds, ^{1}H NMR data of **2**, **3**, **12**, **13**, and **32**, and HPLC charts of representative compounds. This material is available free of charge via the Internet at http://pubs.acs.org.

References

(1) Murphy, P. M.; Baggiolini, M.; Charo I. F.; Herbert, C. A.; Horuk, R.; Matsushima, K.; Miller, L. H.; Oppenheim, J. J.; Power, C. A. International union of pharmacology. XXII. Nomenclature for chemokine receptors. *Pharmacol. Rev.* **2000**, *52*, 145−176.
(2) Mackay, C. R.; Chemokines: immunology's high impact factors. *Nat. Immunol.* **2001**, *2*, 95−101.
(3) Premack, B. A.; Schall, T. J. Chemokine receptors: gateways to inflammation and infection. *Nat. Med.* **1996**, *2*, 1174−1178.
(4) Zlotnik, K.; Yoshie, O. Chemokines: a new classification system and their role in immunity. *Immunity* **2000**, *12*, 121−127.
(5) Bleul, C. C.; Fuhlbrigge, R. C.; Casanovas, J. M.; Aiuti, A.; Springer, T. A. A highly efficacious lymphocyte chemoattractant, stromal cell-derived factor 1 (SDF-1). *J. Exp. Med.* **1996**, *2*, 1101−1109.
(6) Tachibana, K.; Hirota, S.; Iizasa, H.; Yoshida, H.; Kawabata, K.; Kataoka, Y.; Kitamura, Y.; Matsushima, K.; Yoshida, N.; Nishikawa, S.; Kishimoto, T.; Nagasawa, T. The chemokine receptor CXCR4 is essential for vascularization of the gastrointestinal tract. *Nature* **1998**, *393*, 591−594.
(7) Nagasawa, T.; Hirota, S.; Tachibana, K.; Takakura, N.; Nishikawa, S.; Kitamura, Y.; Yoshida, N.; Kikutani, H.; Kishimoto, T. Defects of B-cell limphopoiesis and bone-marrow myelopoiesis in mice lacking the CXC chemokine PBSF/SDF-1. *Nature* **1996**, *382*, 635−638.
(8) Aiuti, A.; Webb, I. J.; Bleul, C.; Springer, T.; Gutierrez-Ramos, J. C. The chemokine SDF-1 is a chemoattractant for human CD34$^+$ hematopoietic progenitor cells and provides a new mechanism to explain the mobilization of CD34$^+$ progenitors to peripheral blood. *J. Exp. Med.* **1997**, *2*, 111−120.
(9) Zhu, Y.; Yu, Y.; Zhang, X. C.; Nagasawa, T.; Wu, J. Y.; Rao, Y. Role of the chemokine SDF-1 as the meningeal attractant for embryonic cerebellar neurons. *Nat. Neurosci.* **2002**, *5*, 719−720.
(10) Stumm, R. K.; Zhou, C.; Ara, T.; Lazarini, F.; Dubois-Dalcq, M.; Nagasawa, T.; Hollt, V.; Schulz, S. CXCR4 regulates interneuron migration in the developing neocortex. *J. Neurosci.* **2003**, *23*, 5123−5130.
(11) Feng, Y.; Broder, C. C.; Kennedy, P. E.; Berger, E. A. HIV-1 entry co-factor: Functional cDNA cloning of a seven-transmembrane G protein-coupled receptor. *Science* **1996**, *272*, 872−877.
(12) Oberlin, E.; Amara, A.; Bachelerie, F.; Bessia, C.; Virelizier, J. L.; Arenzana-Seisdedos, F.; Schwartz, O.; Heard, J. M.; Clark-Lewis, I.; Legler, D. L.; Loetscher, M.; Baggiolini, M.; Moser, B. The CXC chemokine SDF-1 is the ligand for LESTR/fusin and prevents infection by T-cell-line-adapted HIV-1. *Nature* **1996**, *382*, 833−835.
(13) Müller, A.; Homey, B.; Soto, H.; Ge, N.; Catron, D.; Buchanan, M. E.; Mcclanahan, T.; Murphy, E.; Yuan, W.; Wagner, S. M.; Barrera, J. L.; Mohar, A.; Verástegui, E.; Zlotnik, A. Involvement of chemokine receptors in breast cancer metastasis. *Nature* **2001**, *410*, 50−56.
(14) Nanki, T.; Hayashida, K.; El-Gabalawy, H. S.; Suson, S.; Shi, K.; Girschick, H. J., Yavuz, S.; Lipsky, P. E. Stromal cell-derived factor-1-CXC chemokine receptor interactions play a central role in CD4$^+$ T cell accumulation in rheumatoid arthritis synovium. *J. Immunol.* **2000**, *165*, 6590−6598.
(15) Masuda, M.; Nakashima, H.; Ueda, T.; Naba, H.; Ikoma, R.; Otaka, A.; Terakawa, Y.; Tamamura, H.; Ibuka, T.; Murakami, T.; Koyanagi, Y.; Waki, M.; Matsumoto, A.; Yamamoto, N.; Funakoshi, S.; Fujii,

N. A novel anti-HIV synthetic peptide, T-22 ([Tyr^{5,12},Lys^{7}]-polyphemusin II). *Biochem. Biophys. Res. Commun.* **1992**, 189, 845−850.
(16) Tamamura, H.; Xu, Y.; Hattori, T.; Zhang, X.; Arakaki, R.; Kanbara, K.; Omagari, A.; Otaka, A.; Ibuka, T.; Yamamoto, N.; Nakashima, H.; Fujii, N. A low molecular weight inhibitor against the chemokine redeptor CXCR4: a strong anti-HIV peptide T140. *Biochem. Biophys. Res. Commun.* **1998**, *253*, 877−882.
(17) Tamamura, H.; Hori, A.; Kanzaki, N.; Hiramatsu, K.; Mizumoto, M.; Nakashima, H.; Yamamoto, N.; Otaka, A.; Fujii, N. T140 analogues as CXCR4 antagonists identified as anti-metastatic agent in the treatment of breast cancer. *FEBS Lett.* **2003**, *550*, 79−83.
(18) Takenaga, M.; Tamamura, H.; Hiramatsu, K.; Nakamura, N.; Yamaguchi, Y.; Kitagawa, A.; Kawai, S.; Nakashima, H.; Fujii, N.; Igarashi, R. A single treatment with microcapsules containing a CXCR4 antagonist suppressed pulmonary metastasis of murine melanoma. *Biochem. Biophys. Res. Commun.* **2004**, 320, 226−232.
(19) Tamamura, H.; Fujisawa, M.; Hiramatsu, K.; Mizumoto, M.; Nakashima, H.; Yamamoto, N.; Otaka, A.; Fujii, N. Identification of a CXCR4 antagonist, T140 analog, as anti-rheumatoid arthritis agent. *FEBS Lett.* **2004**, *569*, 99−104.
(20) Schols, D.; Struyf, S.; Van Damme, J.; Este, J. A,; Henson, G.; De Clarcq, E. Inhibition of T-tropic HIV strains by selective antagonization of the chemokine receptor CXCR4. *J. Exp. Med.* **1997**, *186*, 1383−1388.
(21) Donzella, G. A.; Schols, D.; Lin, S. W.; Este, J. A.; Nagashima, K. A.; Maddon P. J. AMD3100, a small molecule inhibitor of HIV-1 entry via the CXCR4 co-receptor. *Nat. Med.* **1998**, *4*, 72−76.
(22) Ichiya, K.; Yokoyama-Kumakura, S.; Tanaka, Y.; Tanaka, R.; Hirose, K.; Bannai, K.; Edamatsu, T.; Yanaka, M.; Niitani, Y.; Miyano-Kurosaki, N.; Takaku, H.; Koyanagi, Y.; Yamamoto, N. A duodenally absorbable CXC chemokine receptor 4 antagonist, KRH-1636, exhibits a potent and selective anti-HIV-1 activity. *Proc. Natl. Acad. Sci. U.S.A.* **2003**, *100*, 4185−4190.
(23) Fujii, N.; Oishi, S.; Hiramatsu, K.; Araki, T.; Ueda, S.; Tamamura, H.; Otaka, A.; Kusano, S.; Terakubo, S.; Nakashima, H.; Broach, J. A.; Trent, J. O.; Wang, Z.; Peiper, S. C. Molecular-size reduction of a potent CXCR4-chemokine antagonist using orthogonal combination of conformation- and sequence-based libraries. *Angew. Chem. Int. Ed.* **2003**, *42*, 3251−3253.
(24) Tamamura, H.; Omagari, A.; Oishi, S.; Kanamoto, T.; Yamamoto, N.; Peiper, S. C.; Nakashima, H.; Otaka, A.; Fujii, N. Pharmacophore identification of a specific CXCR4 inhibitor, T140, lead to development of effective anti-HIV agents with very high selectivity indexes. *Bioorg. Med. Chem. Lett.* **2000**, *10*, 2633−2637.
(25) Tamamura, H.; Hiramatsu, K.; Ueda, S.; Wang, Z.; Kusano, S.; Terakubo, S.; Trent, J. O.; Peiper, S. C.; Yamamoto, N.; Nakashima, H.; Otaka, A.; Fujii, N. Stereoselective synthesis of [L-Arg-L/ D-3-(2-naphthyl)alanine]-type (*E*)-alkene dipeptide isosteres and its application to the synthesis and biological evaluation of pseudopeptide analogues of the CXCR4 antagonist FC131. *J. Med. Chem.* **2005**, *48*, 380−391.
(26) Tamamura, H.; Esaka, A.; Ogawa, T.; Araki, T.; Ueda, S.; Wang, Z.; Trent, J. O.; Tsutsumi, H.; Masuno, H.; Nakashima, H.; Yamamoto, N.; Peiper, S. C.; Otaka, A.; Fujii, N. Structure-activity relationship studies on CXCR4 antagonists having cyclic pentapeptide scaffolds. *Org. Biomol. Chem.* **2005**, *3*, 4392−4394.
(27) Tamamura, H.; Araki, T.; Ueda, S.; Wang, Z.; Oishi, S.; Esaka, A.; Trent, J. O.; Nakashima, H.; Yamamoto, N.; Peiper, S. C.; Otaka, A.; Fujii, N. Identification of novel low molecular weight CXCR4 antagonists by structural tuning of cyclic tetrapeptide scaffolds. *J. Med. Chem.* **2005**, *48*, 3280−3289.
(28) Marshall, G. R.; Wu, Y.; Heyden, N. V.; Ratner, L.; Nikiforovich, G. V. Backbone modification of cyclic pentapeptide antagonist of CXCR4. In *Peptides 2004 (Proceedings of 3rd international and 28th European peptide symposium)*; Flegel, M., Fridkin, M., Gilon, C., Slaninova, J., Eds.; Kenes International: Switzerland, 2005; pp 748−749.
(29) Miller, S. C.; Scanlan, T. S. Site-selective N-methylation of peptides on solid support. *J. Am. Chem. Soc.* **1997**, *119*, 2301−2302.
(30) Lin, X.; Dorr, H.; Nuss, J. M. Utilization of Fukuyama's sulfonamide protecting group for the synthesis of *N*-substituted α-amino acids and derivatives. *Tetrahedron Lett.* **2000**, *41*, 3309−3313.
(31) Carpino, L. A.; 1-Hydroxy-7-azabenzotriazole. An efficient peptide coupling additive. *J. Am. Chem. Soc.* **1993**, *115*, 4397−4398.
(32) Bollhagen, R.; Schmiedberger, M.; Barlos. K.; Grell. E. A new reagent for the cleavage of fully protected peptides synthesised on 2-chlorotrityl chloride resin. *J. Chem. Soc., Chem. Commun.* **1994**, 2559−2560.
(33) Haubner, R.; Finsinger, D.; Kessler, H. Stereoisomeric peptide libraries and peptidomimetics for designing selective inhibitors of the $\alpha_v\beta_3$ integrin for a new cancer therapy. *Angew. Chem. Int. Ed. Engl.* **1997**, *36*, 1374−1389.
(34) Toniolo, C. Conformationally restricted peptides through short range cyclization. *Int. J. Pept. Protein Res.* **1990**, *35*, 287−300.
(35) Dechantsreiter, M. A.; Planker, Eckart.; Matha, B.; Lohof, E.; Hölzemann, G.; Jonczyk, A.; Goodman, S. L.; Kessler, H. *N*-Methylated cyclic RGD peptides as highly active and selective $\alpha_v\beta_3$ integrin antagonists. *J. Med. Chem.* **1998**, *42*, 3033−3040.
(36) Rajeswaran, W. G.; Hocart, S. J.; Murphy, W. A.; Taylor, J. E.; Coy, D. H. Highly potent and subtype selective ligand derived by *N*-methyl scan of a somatostatin antagonist. *J. Med. Chem.* **2001**, *44*, 1305−1311.
(37) Erchegyi, J.; Hoeger, C. A.; Low, W.; Hoyer, D.; Waser, B.; Eltschinger, V.; Schaer, J.; Cescato, R.; Reubi, J. C.; Rivier, J. E. Somatostatin receptor 1 selective analogues: 2. N^{α}-Methylated Scan. *J. Med. Chem.* **2005**, *48*, 507−514.
(38) **32** exhibited two sets of signals in ^{1}H NMR spectra. The signals were assigned to *trans*- (69%) and *cis*- (31%) conformers at D-Tyr^1-D-MeArg^2 amide bond. Since backbone conformation and side chain disposition of *cis*-conformer of **32** was apparently different from the parent peptides **2** and **3**, we assumed that the major *trans*-conformer could contribute to the bioactivities of **32**, although contribution of the minor *cis*-conformer cannot be ruled out.
(39) Navenot, J. M.; Wang, Z. X.; Trent, J. O.; Murray, J. L.; Hu, Q. X.; DeLeeuw, L.; Moore, P. S.; Chang, Y.; Peiper, S. C. Molecular anatomy of CCR5 engagement by physiologic and viral chemokines and HIV-1 envelope glycoproteins; Differences in primary structural requirements for RANTES, MIP-1α, and vMIP-II binding. *J. Mol. Biol.* **2001**, *59*, 380−393.

JM0607350

Available online at www.sciencedirect.com
ScienceDirect
ELSEVIER
Biochemical and Biophysical Research Communications 355 (2007) 970–975
BBRC
www.elsevier.com/locate/ybbrc

Rapid hematopoietic progenitor mobilization by sulfated colominic acid

Shiro Kubonishi [a], Tomoko Kikuchi [a], Shinya Yamaguchi [b], Hirokazu Tamamura [c], Nobutaka Fujii [d], Takeshi Watanabe [e], Fernando Arenzana-Seisdedos [f], Kazuma Ikeda [a], Toshimitsu Matsui [g], Mitsune Tanimoto [a], Yoshio Katayama [g,*]

[a] *Hematology, Oncology and Respiratory Medicine, Okayama University Graduate School of Medicine, Dentistry and Pharmaceutical Sciences, Okayama, Japan*
[b] *Marukin Bio Inc., Kyoto, Japan*
[c] *Institute of Biomaterials and Bioengineering, Tokyo Medical and Dental University, Tokyo, Japan*
[d] *Graduate School of Pharmaceutical Sciences, Kyoto University, Kyoto, Japan*
[e] *Research Unit for Immune Surveillance, RIKEN Reserch Center for Allergy and Immunology, Yokohama, Japan*
[f] *United Immunologie Virale, Institute Pasteur, Paris, France*
[g] *Hematology/Oncology, Department of Medicine, Kobe University Graduate School of Medicine, 7-5-1, Kusunoki-cho, Chuo-ku, Kobe 650-0017, Japan*

Received 30 January 2007
Available online 22 February 2007

Abstract

Hematopoietic progenitor cells (HPCs) can be mobilized from bone marrow (BM) to the blood by G-CSF. In this process, CXCR4 and CD26 play critical roles. Sulfated colominic acid (SCA) inhibits HIV entry, the step which requires CXCR4 and CD26 as co-receptors. Thus, we hypothesized that SCA would modulate HPC trafficking. We first found that SCA mobilized HPCs rapidly via CD26-independent mechanism. In vitro progenitor migration toward chemokine SDF-1 was significantly enhanced by SCA, and it was completely abrogated by CXCR4 inhibition. This likely originated from the inhibition of CXCR4 down-regulation after interaction with SDF-1. Serum SDF-1 level increased after SCA injection, whereas no change was observed in BM and bone. These results suggest that SCA induces HPC mobilization by modulating CXCR4 function resulting in attraction toward increased SDF-1 in the circulation. Furthermore, we confirmed an additive effect with G-CSF in mobilization. SCA may provide an efficacy in clinical mobilization.

Keywords: Hematopoietic stem/progenitor cells; SDF-1/CXCL12; CXCR4; Mobilization; Sulfated colominic acid; G-CSF

Hematopoietic stem/progenitor cells (HSCs/HPCs) can be mobilized from the bone marrow (BM) compartment to the blood by various molecules such as cytokines, chemokines and chemotherapeutic agents [1]. Mobilized peripheral blood HSCs/HPCs, instead of BM, have become the principal cellular source for reconstitution of the hematopoietic system following myeloablative and non-myeloablative therapy. Granulocyte-colony stimulating factor (G-CSF) is most widely used agent in clinic for mobilization [2]. The advantages of G-CSF are that (1) the mobilization efficiency is relatively potent and predictable, (2) the safety to donor is established. However, several problems are remained to be solved such as (1) necessity of at least 4-day administration of high dose of G-CSF, (2) high cost of this recombinant protein, (3) bone pain, headache and fever during administration, (4) a certain population of unpredictable poor mobilizers [3]. It is important to characterize new agents which can induce rapid and efficient mobilization to overcome these problems.

The investigation for mechanistic insights of G-CSF-induced mobilization has been focused on mainly chemokine SDF-1/CXCL12 in the BM and its cognate receptor CXCR4 on HSCs/HPCs. It has been reported that proteolytic or transcriptional down-regulation of SDF-1 in the

* Corresponding author. Fax: +81 78 382 5899.
E-mail address: katayama@med.kobe-u.ac.jp (Y. Katayama).

0006-291X/$ - see front matter © 2007 Elsevier Inc. All rights reserved.
doi:10.1016/j.bbrc.2007.02.069

BM may be the main reason for the loss of the retention signal resulting in release of HSCs/HPCs to the periphery [4–7]. Moreover, treatment with AMD3100, a specific CXCR4 antagonist, induces rapid and robust HPC mobilization [8]. Interestingly, a membrane-bound extracellular peptidase CD26 (dipeptidylpeptidase IV [DPPIV]) that cleaves dipeptides from the N-terminus of polypeptides including SDF-1, has been reported to be expressed on HPCs and indispensable for G-CSF-induced mobilization [9,10]. Collectively, these data strongly suggest that the modulation of SDF-1 oriented molecules, such as SDF-1 itself produced in microenvironment and CXCR4/CD26 expressed on HSCs/HPCs, is crucial for mobilization.

Colominic acid (CA) is a homopolymer of *N*-acetylneuraminic acid (sialic acid) containing α-2,8-ketosidic linkages between the sugar moieties [11]. It has been reported that sulfated colominic acid (SCA, structure is shown in Supplemental Fig. 1S) exhibits anti-HIV activity [12], and suppresses scrapie prion protein (PrP^{Sc}) and HIV-1 gp-120-induced neuronal cell death [13]. Since recent accumulating evidences suggest that CXCR4 and CD26 play critical roles in HIV entry as co-receptors [14,15], it is possible that SCA modulates CXCR4 and/or CD26. Thus, we hypothesized that SCA would regulate HSC/HPC trafficking by modulating SDF-1 oriented molecules.

Materials and methods

Mice and cell lines. C57BL/6, DBA/2 and Balb/c mice were purchased from Charles River Japan (Tsukuba, Japan). C57BL/6-CD45.1 congenic mice were purchased from Charles River Laboratories (Frederick Cancer Research Center, Frederick, MD). CD26-deficient mice were generated by gene targeting [16] and were backcrossed 10 generations into Balb/c background. All animals used in this study were matched for sex and age in each experiment for the comparison purpose (7–12 week old). All experiments involving animals were performed under the auspices of the Institutional Animal Care and Research Advisory Committee at the Department of Animal Resources, Okayama University Advanced Science Research Center. FDCP-mix mouse progenitor cell line was purchased from DSMZ (German Collection of Microorganisms and Cell Cultures, Braunschweig, Germany).

Mobilization of hematopoietic stem/progenitor cells. SCA and CA were prepared in Marukin Bio, Inc. (Kyoto, Japan) as previously described [12]. Endotoxin in SCA solution was under detection level by Toxicolor LS-20 (Seikagaku, Tokyo, Japan). For mobilization studies, mice were injected intravenously with a single dose of CA or SCA diluted in phosphate-buffered saline (PBS) (100 mg/kg). Mice were bled at various time points post-administration of SCA. Since mobilization effect peaked at 30 min, mice were treated with CA or SCA 30 min prior to harvesting blood in the following mobilization studies. Inhibition of endogenous CD26/DPPIV activity was accomplished by intraperitoneal injection of 30 μmol Diprotin A (Sigma, St. Louis, MO) 30 min prior to SCA injection. For G-CSF-induced mobilization, mice were subcutaneously injected with recombinant human G-CSF (filgrastim, Kirin Brewery, Tokyo, Japan, 250 μg/kg/day, every 12 h, eight divided doses) in PBS supplemented with 0.1% BSA and were bled 3 h following the last dose of G-CSF.

Long-term competitive reconstitution. Stem cell activities of blood mobilized by 2 day-G-CSF + single dose of SCA and by 4 day-G-CSF were compared by long-term competitive reconstitution. C57BL/6 mice (CD45.2) and Ly5.2 congenic mice (CD45.1) were treated with 2 day-G-CSF+SCA and 4 day-G-CSF, respectively. The number of CFU-Cs in the blood obtained from each donor was assessed as described above. As predicted, the average ratio of CFU-Cs in the same volume of blood from each group was 49:51, respectively ($n = 5$). The same volume (150 μl) of blood from a pair of donor mice were mixed and injected into the tail vein of a lethally (13 Gy, two split doses) irradiated CD45.1 recipient mouse. The proportion of peripheral blood leukocytes bearing CD45.1 or CD45.2 antigen was determined monthly after transplantation by flow cytometry as previously described [17].

Chemotaxis assay. IMDM supplemented with 0.5% BSA with or without 200 ng/ml rhSDF-1α (R&D Systems, Minneapolis, MN) was added to the lower chamber of 24-well transwell (pore size, 5 μm; Corning, NY). Cells were treated with PBS or 1 mg/ml SCA for 30 min on ice and washed twice with PBS and once with IMDM + 0.5% BSA. We chose this concentration because it was predicted by calculation in the mouse blood immediately after injection of 100 mg/kg SCA. Then, 1×10^6 cells with or without 10^{-7} M 4F-Benzonyl-TN14003 (a CXCR4 inhibitor) [18] or 400 μM NSC23766 (a Rac inhibitor) [19] in IMDM + 0.5% BSA were loaded to the upper chamber and were allowed to migrate for 3 h at 37 °C. Migrated cells were collected from the lower chamber and counted using a hemocytometer or assayed for CFU-C.

Antibodies, flow cytometry, colony-forming units in culture (CFU-C) assay, ELISA, statistics. These methods can be found in online Supplemental materials.

Results

SCA induces rapid hematopoietic progenitor mobilization

First, we injected SCA 100 mg/kg i.v. into C57BL/6 mice, and WBC count and the number of CFU-Cs in the blood were assessed. As shown in Fig. 1A, WBC was increased 3.3-fold (peaked at 60 min, $n = 6$–9, $p < 0.01$), and the number of CFU-C was increased 5.1-fold (peaked at 30 min, $n = 9$–12, $p < 0.01$) following injection, and returned to baseline by 5 h. It is well known that broad variability exists in mobilization of HSCs/HPCs in different strains of mice [20]. Thus, we compared the mobilizing capability of SCA in C57BL/6 mice which respond poorly to G-CSF and DBA/2 mice which are relatively good mobilizers [20]. As shown in Fig. 1B, HPC mobilization with single administration of 100 mg/kg SCA was greater in DBA/2 compared with C57BL/6 mice, displaying a similar phenomenon as G-CSF-induced mobilization. We also confirmed that SCA mobilizes HPCs in dose dependent manner up to 100 mg/kg (Fig. 1C). To investigate whether the sulfation is important for SCA-induced HPC mobilization, DBA/2 mice were treated with single-dose (100 mg/kg) of CA or SCA. As shown in Fig. 1D, CA displayed no mobilization, suggesting that the sulfation of CA is critical for mobilization activity.

CD26/dipeptidyl peptidase (DPPIV) is not required for SCA-induced mobilization

It has been reported that CD26/DPPIV [9,10] and chemokine SDF-1/receptor CXCR4 axis [5,6] play critical roles in G-CSF-induced mobilization. Since CD26/DPPIV and CXCR4 are co-modulated in HIV entry [15] and SCA has anti-HIV activity [12], we hypothesized that SCA might modulate CD26 and/or CXCR4 to induce HPC mobilization. We first focused on CD26/DPPIV. As shown in

Fig. 1E and F, pre-treatment of DBA/2 mice with a CD26 inhibitor Diprotin A showed no inhibitory effect in HPC mobilization whereas it significantly inhibited the increase of leukocytes ($n = 3$–5, $p < 0.01$), suggesting different requirement of DPPIV activity for SCA-induced peripheralization of mature and immature hematopoietic cells. Although not as drastic as previously reported probably due to different genetic background [9,10], G-CSF-induced mobilization in CD26-deficient (CD26−/−) Balb/c mice was reduced compared to that in wild-type (WT) control (Fig. 1G, $n = 3$–6, $p < 0.05$). Whereas, SCA-induced mobilization in CD26−/− mice was similar to that in WT control (Fig. 1H, $n = 3$–6). These results suggest that, in contrast to G-CSF-induced mobilization, CD26 is dispensable for SCA action.

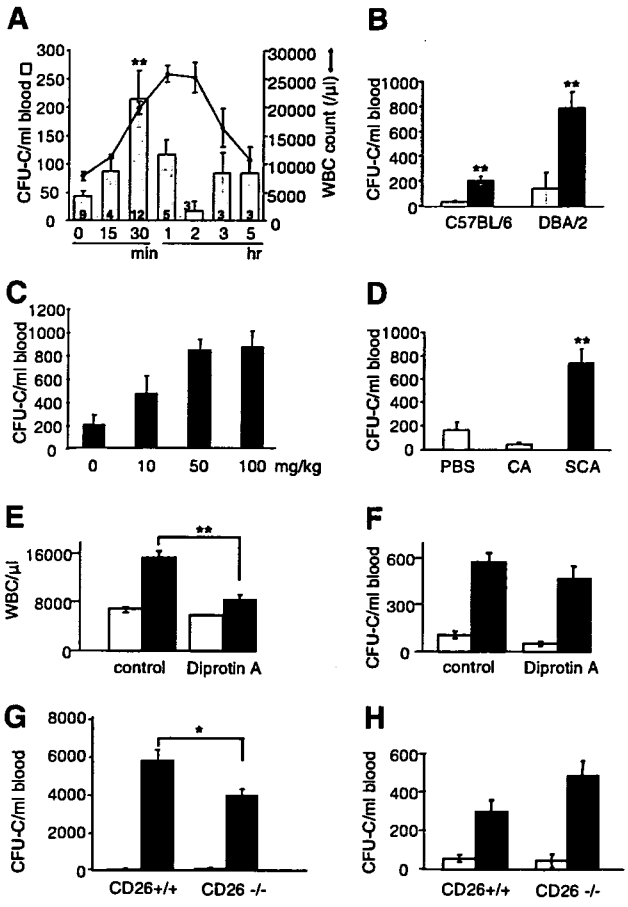

Fig. 1. SCA induces progenitor mobilization via CD26-independent mechanism (A) C57BL/6 mice were injected i.v. with 100 mg/kg SCA and bled at the indicated times. Number of treated mice is listed within the bar. Blood was assayed for CFU-C (bars) or WBC (line). (B) C57BL/6 or DBA/2 mice were treated with PBS (white bar) or 100 mg/kg SCA (black bar) and bled after 30 min, $n = 3$–7. (C) DBA/2 mice were treated with the indicated dose of SCA, $n = 3$–7. (D) DBA/2 mice were treated with PBS or 100 mg/kg colominic acid (CA) or 100 mg/kg SCA, $n = 7$–12. (E,F) Inhibition of CD26 by a CD26 inhibitor Diprotin A. Thirty minutes after pretreatment with PBS or 30 μmol Diprotin A (i.p.), DBA/2 mice were treated with PBS (white bar) or 100 mg/kg SCA (black bar) and bled after 30 min. Blood was assayed for (E) WBC and (F) CFU-C. $n = 3$–5. (G) Wild-type (CD26+/+) and CD26-deficient (CD26−/−) mice were treated with either PBS containing 0.1% BSA (white bar) or 250 μg/kg/day (two divided doses) G-CSF (black bar) for four days. Three hours after the final dose of G-CSF, mice were bled to assess CFU-C numbers. $n = 3$–6. (H) CD26+/+ and CD26−/− mice were injected i.v. with either PBS (white bar) or 100 mg/kg SCA (black bar), and bled after 30 min. Blood was assayed for CFU-C. $n = 4$–6. $^{*}p < 0.05$, $^{**}p < 0.01$ compared to 0 min (A) or control groups, or between indicated two groups.

SCA enhances CXCR4 function on hematopoietic progenitors

Next, to assess the functional alteration of CXCR4, we tested the migration potential of SCA-treated FDCP-mix,

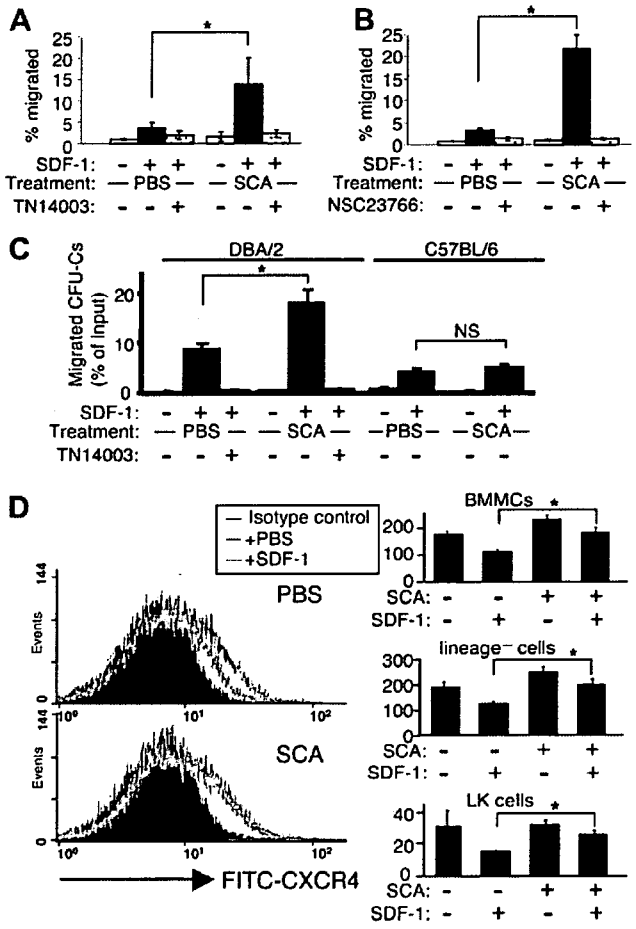

Fig. 2. SCA enhances CXCR4 function on progenitors. (A,B) FDCP-mix cells treated with PBS or SCA ± (A) 4F-benzoyl-TN14003 (a CXCR4 inhibitor) or (B) NSC23766 (a Rac inhibitor) were tested in a transwell for their migration toward 200 ng/ml SDF-1. $n = 3$–8. (C) Bone marrow mononuclear cells (BMMCs) of DBA/2 or C57BL/6 mice were treated with PBS or SCA ± 4F-benzoyl-TN14003 and tested in a transwell for their migration toward 200 ng/ml SDF-1. Input and migrated cells were assayed for CFU-C. $n = 3$–8. (D) Surface CXCR4 expression in BMMCs of DBA/2 mice. BMMCs pretreated with PBS or 1 mg/ml SCA were incubated with PBS or 200 ng/ml SDF-1α. Histograms show immunofluorescence detection of isotype control (black histogram), or CXCR4 (red line; incubated with PBS, green line; incubated with SDF-1α) in lineage^{-} c-kit^{+} (LK) fraction. Bar graphs show geometric mean fluorescence intensity after subtraction of isotype control value. $^{*}p < 0.05$ between indicated two groups. NS, not significant.

a mouse progenitor cell line, toward SDF-1 in a transwell. SCA treatment strongly enhanced FDCP-mix migration toward SDF-1 (Fig. 2A, $n = 8$, $p < 0.05$) which was completely blocked by the presence of a CXCR4 inhibitor 4F-Benzonyl-TN14003 (Fig. 2A) or a Rac inhibitor NSC23766 (Fig. 2B). These results suggest that SCA may enhance the CXCR4 signaling including the Rac activation in HPCs. Then, we investigated the effects of SCA on primary HPCs. As shown in Fig. 2C, SCA significantly enhanced migration of primary BM CFU-Cs from DBA/2 mice. This effect was completely abrogated by CXCR4 inhibitor. In contrast, in C57BL/6 mice, baseline efficiency of CFU-C migration was lower than DBA/2 and SCA showed no effect (Fig. 2C). This may explain, at least partially, the reason for poor mobilization in C57BL/6 mice. Surface expression of CXCR4 was not significantly increased by SCA treatment in BMMCs, lineage- cells, and lineage$^-$c-kit$^+$ (LK) cells (Fig. 2D). Rather, SCA completely inhibited the down-regulation of CXCR4 upon interaction with SDF-1 (Fig. 2D). These results suggest that SCA enhances CXCR4 function on HPCs by stabilizing its expression on cell surface and inducing continuous maximum signaling in the presence of the ligand.

SCA increases SDF-1 level in peripheral blood but does not decrease in BM or bone

After injection of fucoidan, a natural sulfated fucose polymer extracted from seaweed, SDF-1 level in serum increases whereas its level in BM decreases drastically [21], suggesting that fucoidan sweeps SDF-1 in BM and takes it into the circulation. We then evaluated the alteration of SDF-1 distribution by evaluating its levels in serum, BM, and bone after SCA injection. We used two different capture antibodies for ELISA, MAB350 whose binding site on SDF-1 molecule has not been determined (R&D systems) and K15C which detects only non-truncated active SDF-1 [22]. As shown in Fig. 3A, serum SDF-1 level of DBA/2 mice 30 min after SCA injection was detected at similar levels between MAB350 and K15C, and was increased approximately five times compared to PBS-injected group ($n = 5$, $p < 0.0001$). An increase of serum SDF-1 level was also observed in C57BL/6 mice, but to the lesser extent (Fig. 3A). This increased SDF-1 did not come from BM cavity and not

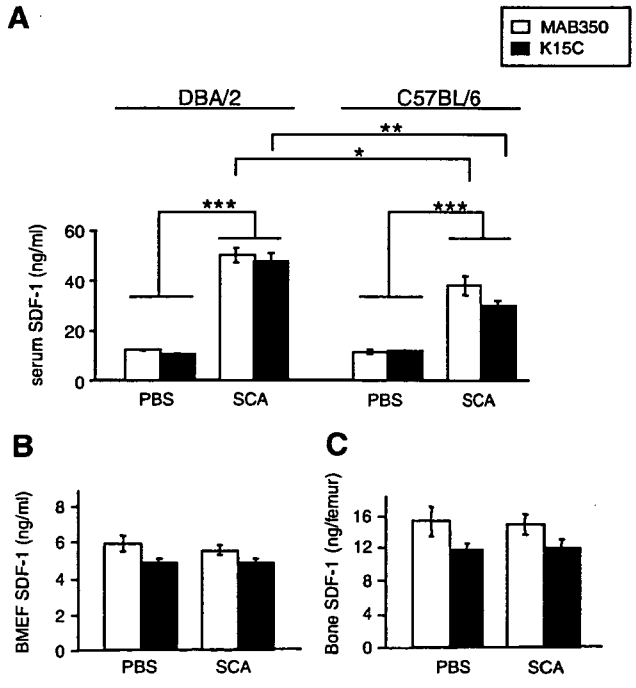

Fig. 3. SDF-1 levels after SCA treatment. SDF-1 levels were measured by ELISA in (A) serum from DBA/2 and C57BL/6 mice, (B) bone marrow extracellular fluid (BMEF) from DBA/2 mice, (C) bone from DBA/2 mice after treatment with PBS or 100 mg/kg SCA. $n = 4$–5 per group, $^*p < 0.05$, $^{**}p < 0.01$, $^{***}p < 0.0001$.

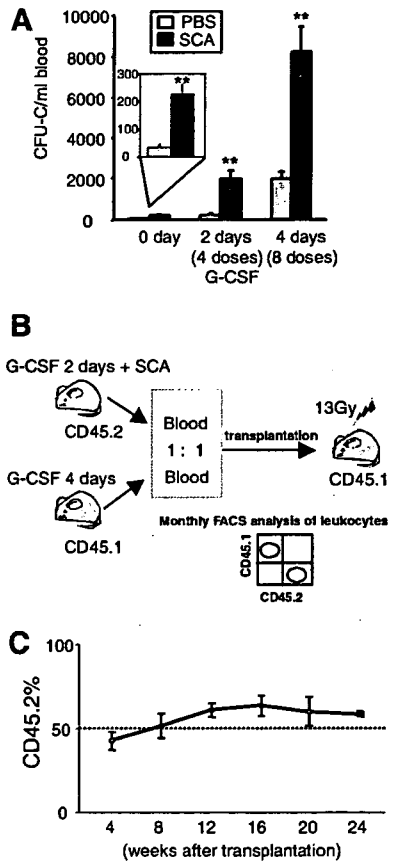

Fig. 4. SCA cooperates with G-CSF in progenitor and stem cell mobilization. (A) C57BL/6 mice were treated with 250 μg/kg/day (two divided doses) G-CSF for the indicated days. Three hours after the final dose of G-CSF, mice were bled to assess CFU-C numbers. PBS or 100 mg/kg SCA was injected 30 min prior to bleeding. $n = 5$–6, $^{**}p < 0.001$ compared with the PBS injected group at each time point. (B) Competitive reconstitution. Lethally irradiated Ly5.2 (CD45.1+) mice were injected with blood mixture consisted of the same volume of 2 day-G-CSF+SCA-mobilized blood from C57BL/6 (CD45.2+) mice and 4 day-G-CSF-mobilized blood from Ly5.2 (CD45.1+) mice. Recipient mice were bled monthly and the percentage of CD45.1/CD45.2 was assessed. (C) Chimerism of peripheral blood leukocytes. $n = 5$ at up to 12 weeks, $n = 3$–4 at later periods.

even bone, since SDF-1 protein levels in bone marrow extracellular fluid (BMEF) and bone were unchanged during SCA treatment (Fig. 3B and C). These results suggest that SCA may induce mobilization by not only enhancing CXCR4 function on HPCs but also by the increased SDF-1 in the circulation.

SCA cooperates with G-CSF in stem and progenitor mobilization

To test the potential clinical application, the mobilizing efficiency of SCA in combination with G-CSF was assessed. C57BL/6 mice were injected with G-CSF for 2 days or 4 days, and 30 min prior to bleeding mice were injected with single dose of vehicle or SCA. As shown in Fig. 4A, G-CSF-induced HPC mobilization was strongly enhanced by the addition of single dose of SCA ($n = 5$–6, $p < 0.001$). Since 2 day-G-CSF+SCA showed equivalent progenitor mobilization efficiency to that of full-term (4 days) G-CSF, we compared the stem cell activities in mobilized blood of these two protocols. Same volume of blood from C57BL/6 mice (CD45.2) treated with 2 day-G-CSF+SCA and Ly5.2 mice (CD45.1) treated with 4 day-G-CSF were mixed, and injected into lethally irradiated Ly5.2 (CD45.1) mice (Fig. 4B). As shown in Fig. 4C, the percentage of peripheral blood leukocytes derived from engrafted stem cells originated from CD45.2+ donor was more than 50% for 24 weeks after transplantation. This suggests that 2 day administration of G-CSF together with single dose of SCA mobilizes long-term reconstituting stem cells as efficient as usual G-CSF protocol and may be sufficient for clinical mobilization.

Discussion

Here, we demonstrated that a synthetic polysaccharide SCA rapidly mobilizes HSCs/HPCs by inducing two concurrent events, (1) enhancement of CXCR4 function (inhibition of ligand-induced down-regulation) and (2) increment of SDF-1 concentration in the blood.

Fucoidan can also mobilize HSCs/HPCs [23,24], and binds L-selectin on hematopoietic cells resulting in up-regulation of surface CXCR4 expression [25]. However, we confirmed that SCA does not bind L-selectin (Supplemental Fig. 2S), suggesting that SCA and fucoidan modulate CXCR4 function in different mechanism.

It has been reported that SDF-1 level in BM is sharply decreased after fucoidan treatment, suggesting that increased serum SDF-1 was brought from BM parenchyma [21]. However, following SCA injection, SDF-1 levels in BM and even bone were not altered (Fig. 3). This suggests that increased serum SDF-1 after SCA administration does not originate from BM cavity but perhaps from extramedullary sites. Recently, Kiel et al. have reported that hematopoietic stem cell niche is located not only at osteoblastic area near the endosteum but also at the vascular area [26]. Since our ELISA data showed that SDF-1 levels in BM parenchyma and bone were not altered after SCA treatment, it is likely that stem/progenitor cells located at osteoblastic area cannot egress from BM even if CXCR4 function of these cells is up-regulated. One possible scenario for SCA mobilization is that stem/progenitor cells located at the vascular area are strongly attracted by rapidly increased serum SDF-1 via enhanced CXCR4 function on the surface of these cells.

According to the cooperative effect between G-CSF and SCA (Fig. 4), it may be possible to shorten the mobilization protocol in clinic. This would be a great benefit for cost effectiveness and the reduction of side effects. Furthermore, addition of SCA to full-term G-CSF may overcome poor mobilization cases in a certain population of healthy donors and in patients with some malignancies such as multiple myeloma. The mechanism of this cooperative action remains to be elucidated.

Modulation of SDF-1-CXCR4 axis is critical in controlling the travel of CXCR4 expressing cells. SCA may be useful not only in HSC mobilization but also in targeting cancer stem cells which express CXCR4 [27].

Acknowledgment

This work was supported in part by the Ministry of Education, Culture, Sports, Science and Technology (Grant No. 17790644 to Y.K.).

Appendix A. Supplementary data

Supplementary data associated with this article can be found, in the online version, at doi:10.1016/j.bbrc.2007.02.069.

References

[1] T. Lapidot, I. Petit, Current understanding of stem cell mobilization: the roles of chemokines, proteolytic enzymes, adhesion molecules, cytokines, and stromal cells, Exp. Hematol. 30 (2002) 973–981.
[2] L.B. To, D.N. Haylock, P.J. Simmons, C.A. Juttner, The biology and clinical uses of blood stem cells, Blood 89 (1997) 2233–2258.
[3] S. Fu, J. Liesveld, Mobilization of hematopoietic stem cells, Blood Rev. 14 (2000) 205–218.
[4] Y. Katayama, M. Battista, W.M. Kao, A. Hidalgo, A.J. Peired, S.A. Thomas, P.S. Frenette, Signals from the sympathetic nervous system regulate hematopoietic stem cell egress from bone marrow, Cell 124 (2006) 407–421.
[5] J.P. Levesque, J. Hendy, Y. Takamatsu, P.J. Simmons, L.J. Bendall, Disruption of the CXCR4/CXCL12 chemotactic interaction during hematopoietic stem cell mobilization induced by GCSF or cyclophosphamide, J. Clin. Invest. 111 (2003) 187–196.
[6] I. Petit, M. Szyper-Kravitz, A. Nagler, M. Lahav, A. Peled, L. Habler, T. Ponomaryov, R.S. Taichman, F. Arenzana-Seisdedos, N. Fujii, J. Sandbank, D. Zipori, T. Lapidot, G-CSF induces stem cell mobilization by decreasing bone marrow SDF-1 and up-regulating CXCR4, Nat. Immunol. 3 (2002) 687–694.
[7] C.L. Semerad, M.J. Christopher, F. Liu, B. Short, P.J. Simmons, I. Winkler, J.P. Levesque, J. Chappel, F.P. Ross, D.C. Link, G-CSF potently inhibits osteoblast activity and CXCL12 mRNA expression in the bone marrow, Blood (2005).

[8] H.E. Broxmeyer, C.M. Orschell, D.W. Clapp, G. Hangoc, S. Cooper, P.A. Plett, W.C. Liles, X. Li, B. Graham-Evans, T.B. Campbell, G. Calandra, G. Bridger, D.C. Dale, E.F. Srour, Rapid mobilization of murine and human hematopoietic stem and progenitor cells with AMD3100, a CXCR4 antagonist, J. Exp. Med. 201 (2005) 1307–1318.
[9] K.W. Christopherson 2nd, S. Cooper, H.E. Broxmeyer, Cell surface peptidase CD26/DPPIV mediates G-CSF mobilization of mouse progenitor cells, Blood 101 (2003) 4680–4686.
[10] K.W. Christopherson, S. Cooper, G. Hangoc, H.E. Broxmeyer, CD26 is essential for normal G-CSF-induced progenitor cell mobilization as determined by CD26−/− mice, Exp Hematol 31 (2003) 1126–1134.
[11] E.J. McGuire, S.B. Binkley, The structure and chemistry of colominic acid, Biochemistry 3 (1964) 247–251.
[12] D.W. Yang, Y. Ohta, S. Yamaguchi, Y. Tsukada, Y. Haraguchi, H. Hoshino, H. Amagai, I. Kobayashi, Sulfated colominic acid: an antiviral agent that inhibits the human immunodeficiency virus type 1 in vitro, Antiviral Res. 31 (1996) 95–104.
[13] H. Ushijima, S. Perovic, J. Leuck, P.G. Rytik, W.E. Muller, H.C. Schroder, Suppression of PrP(Sc)- and HIV-1 gp120 induced neuronal cell death by sulfated colominic acid, J. Neurovirol. 5 (1999) 289–299.
[14] E.A. Berger, P.M. Murphy, J.M. Farber, Chemokine receptors as HIV-1 coreceptors: roles in viral entry, tropism, and disease, Annu. Rev. Immunol. 17 (1999) 657–700.
[15] C. Herrera, C. Morimoto, J. Blanco, J. Mallol, F. Arenzana, C. Lluis, R. Franco, Comodulation of CXCR4 and CD26 in human lymphocytes, J. Biol. Chem. 276 (2001) 19532–19539.
[16] D. Marguet, L. Baggio, T. Kobayashi, A.M. Bernard, M. Pierres, P.F. Nielsen, U. Ribel, T. Watanabe, D.J. Drucker, N. Wagtmann, Enhanced insulin secretion and improved glucose tolerance in mice lacking CD26, Proc. Natl. Acad. Sci. USA 97 (2000) 6874–6879.
[17] Y. Katayama, A. Hidalgo, B.C. Furie, D. Vestweber, B. Furie, P.S. Frenette, PSGL-1 participates in E-selectin-mediated progenitor homing to bone marrow: evidence for cooperation between E-selectin ligands and alpha4 integrin, Blood 102 (2003) 2060–2067.
[18] H. Tamamura, M. Fujisawa, K. Hiramatsu, M. Mizumoto, H. Nakashima, N. Yamamoto, A. Otaka, N. Fujii, Identification of a CXCR4 antagonist, a T140 analog, as an anti-rheumatoid arthritis agent, FEBS Lett. 569 (2004) 99–104.
[19] Y. Gao, J.B. Dickerson, F. Guo, J. Zheng, Y. Zheng, Rational design and characterization of a Rac GTPase-specific small molecule inhibitor, Proc. Natl. Acad. Sci. USA 101 (2004) 7618–7623.
[20] A.W. Roberts, S. Foote, W.S. Alexander, C. Scott, L. Robb, D. Metcalf, Genetic influences determining progenitor cell mobilization and leukocytosis induced by granulocyte colony-stimulating factor, Blood 89 (1997) 2736–2744.
[21] E.A. Sweeney, H. Lortat-Jacob, G.V. Priestley, B. Nakamoto, T. Papayannopoulou, Sulfated polysaccharides increase plasma levels of SDF-1 in monkeys and mice: involvement in mobilization of stem/progenitor cells, Blood 99 (2002) 44–51.
[22] A. Amara, O. Lorthioir, A. Valenzuela, A. Magerus, M. Thelen, M. Montes, J.L. Virelizier, M. Delepierre, F. Baleux, H. Lortat-Jacob, F. Arenzana-Seisdedos, Stromal cell-derived factor-1alpha associates with heparan sulfates through the first beta-strand of the chemokine, J. Biol. Chem. 274 (1999) 23916–23925.
[23] P.S. Frenette, L. Weiss, Sulfated glycans induce rapid hematopoietic progenitor cell mobilization: evidence for selectin-dependent and independent mechanisms, Blood 96 (2000) 2460–2468.
[24] E.A. Sweeney, G.V. Priestley, B. Nakamoto, R.G. Collins, A.L. Beaudet, T. Papayannopoulou, Mobilization of stem/progenitor cells by sulfated polysaccharides does not require selectin presence, Proc. Natl. Acad. Sci. USA 97 (2000) 6544–6549.
[25] Z. Ding, T.B. Issekutz, G.P. Downey, T.K. Waddell, L-selectin stimulation enhances functional expression of surface CXCR4 in lymphocytes: implications for cellular activation during adhesion and migration, Blood 101 (2003) 4245–4252.
[26] M.J. Kiel, O.H. Yilmaz, T. Iwashita, O.H. Yilmaz, C. Terhorst, S.J. Morrison, SLAM family receptors distinguish hematopoietic stem and progenitor cells and reveal endothelial niches for stem cells, Cell 121 (2005) 1109–1121.
[27] J.A. Burger, T.J. Kipps, CXCR4: a key receptor in the crosstalk between tumor cells and their microenvironment, Blood 107 (2006) 1761–1767.

Available online at www.sciencedirect.com
ScienceDirect
ELSEVIER
Biochemical and Biophysical Research Communications 361 (2007) 1012–1016
BBRC
www.elsevier.com/locate/ybbrc

CXCR4 engagement promotes dendritic cell survival and maturation

Kenji Kabashima [a,*], Kazunari Sugita [a], Noriko Shiraishi [a], Hirokazu Tamamura [b], Nobutaka Fujii [c], Yoshiki Tokura [a]

[a] *Department of Dermatology, University of Occupational and Environmental Health, 1-1 Iseigaoka, Yahatanishi-ku, Kitakyushu 807-8555, Japan*
[b] *Institute of Biomaterials and Bioengineering, Tokyo Medical and Dental University, Chiyoda-ku, Tokyo 101-0062, Japan*
[c] *Graduate School of Pharmaceutical Sciences, Kyoto University, Sakyo-ku, Kyoto 606-8501, Japan*

Received 14 July 2007
Available online 30 July 2007

Abstract

It has been reported that human monocyte derived-dendritic cells (DCs) express CXCR4, responsible for chemotaxis to CXCL12. However, it remains unknown whether CXCR4 is involved in other functions of DCs. Initially, we found that CXCR4 was expressed on bone marrow-derived DCs (BMDCs). The addition of specific CXCR4 antagonist, 4-F-Benzoyl-TN14003, to the culture of mouse BMDCs decreased their number, especially the mature subset of them. The similar effect was found on the number of Langerhans cells (LCs) but not keratinocytes among epidermal cell suspensions. Since LCs are incapable of proliferating in vitro, these results indicate that CXCR4 engagement is important for not only maturation but also survival of DCs. Consistently, the dinitrobenzene sulfonic acid-induced, antigen-specific in vitro proliferation of previously sensitized lymph node cells was enhanced by CXCL12, and suppressed by CXCR4 antagonist. These findings suggest that CXCL12–CXCR4 engagement enhances DC maturation and survival to initiate acquired immune response.

Keywords: Langerhans cell; Dendritic cell; Maturation; Survival; Antagonist; CXCR4; CXCL12; Proliferation

Dendritic cells (DCs) are potent antigen-presenting cells in the immune system especially for T cell activation and maturation [1,2]. It is well established that DC maturation is induced by cytokines, such as tumor necrosis factor (TNF)-α and interleukin (IL)-1β, pathogens, lipopolysaccharide (LPS), and CD40 ligand [1]. Chemokines were originally known as chemoattractant, but they have currently been evaluated as one of the important candidates for modulators of DC functions [3].

It was reported that the maturation of human monocyte-derived DCs by LPS, TNF-α or CD40L resulted in enhanced expression of CCR7 and CXCR4 [4]. Although the roles of CCR7 on DCs have been well characterized [3], those of CXCR4 remain largely unknown except that CXCR4 signaling promotes chemotaxis to its ligand, CXCL12 (stromal-cell derived factor-1; SDF-1α) in vitro and in vivo [5–7].

In light of the emerging significance of chemokine systems in DC biology, we examined the hypothesis that the CXCL12–CXCR4 engagement influences DC functions as well as chemotaxis. We found that CXCR4 was expressed on murine bone marrow-derived DCs (BMDCs) and epidermal Langerhans cells (LCs), that CXCL12 was produced by BMDCs, and that CXCR4 signaling promotes DC maturation and survival.

Materials and methods

Animals and reagent. Eight weeks old female C57BL/6 (B6) mice were purchased from Japan SLC (Hamamatsu, Japan) and maintained on a 12-h light/dark cycle under specific pathogen-free conditions. All protocols were approved by the Institutional Animal Care and Use Committee of the University of Occupational and Environmental Health.

For CXCR4 antagonist treatment, 4F-Benzoyl-TN14003 was used as CXCR4 antagonist [8,9]. No toxicity of CXCR4 antagonist was observed at 5 μM as reported previously [10], and the selectivity of the antagonist

* Corresponding author. Fax: +81 93 6910907.
E-mail address: kkabashi@med.uoeh-u.ac.jp (K. Kabashima).

0006-291X/$ - see front matter © 2007 Elsevier Inc. All rights reserved.
doi:10.1016/j.bbrc.2007.07.128

was confirmed by the absence of significant inhibition against Ca^{2+} mobilization induced by MIP-1α stimulation through CCR5 ($IC_{50} = 22$ μM) and against Ca^{2+} mobilization induced by sphingosine-1-phosphate stimulation through EDG3 ($IC_{50} > 30$ μM) by the treatment of CXCR4 antagonist (data not shown).

Cell preparation and cultures. RPMI-1640 (Sigma, St. Louis, MO) containing 10% heat-inactivated fetal calf serum (Invitrogen, Carlsbad, CA), 5×10^{-5} M 2-mercaptoethanol, 2 mM L-glutamine, 25 mM Hepes (Cellgro, Herndon, VA), 1 mM nonessential amino acids, 1 mM sodium pyruvate, 100 U/ml penicillin, and 100 μg/ml streptomycin was used as culture medium otherwise stated. BMDC culture was performed as described [11]. In brief, 5×10^6 BM cells were cultured in 10 cm tissue culture dishes in 10 ml of medium supplemented with 10 ng/ml recombinant murine GM-CSF (PeproTech, Rocky Hill, NJ) for 5 days. Loosely adherent cells were harvested at day 5 and incubated at 1×10^6/ml with or without CXCR4 antagonist in the presence or absence of GM-CSF for another 2 days. The CXCL12 amounts in the culture supernatants were measured with an ELISA kit (R&D systems, Minneapolis, MN) as manufacturer's protocol. Epidermal cell suspensions were obtained from the earlobes of mice with trypsin treatment and cultured without FCS for 48 h [12,13].

Flow cytometry. For flow cytometry, cells were prepared and analyzed with FACSCanto (BD Biosciences) and FlowJo software (TreeStar, San Carlos, CA) [14]. Antibodies (Abs) used were: phycoerythrin (PE)-conjugated anti-CXCR4 (2B11; BD Biosciences) and isotype matched control IgGs, FITC-conjugated anti CD54 Ab, PE-conjugated anti C86 Ab, PE-Cy5-conjugated anti-MHC class II Ab, and allophycocyanin (APC)-conjugated anti-CD11c Ab (all from BD Biosciences).

Hapten specific T cell proliferation model. For 2,4-dinitrobenzene sulfonic acid (DNBS)-dependent in vitro T cell proliferation, cells were prepared from draining axillary and inguinal lymph nodes of mice 5 days after sensitization on abdomen with 25 μl of 0.5% 2,4-dinitro-1-fluorobenzene (DNFB) in 4:1 (v/v) acetone/olive oil. Cells (4×10^5/well of 96 well plates) were cultured for 3 days with DNBS (50 μg/ml), a water-soluble compound with the same antigenicity as DNFB, in the presence or absence of CXCL12 (R&D systems) and were pulsed with 1 μCi ^3H thymidine for the last 24 h of culture.

Statistical analysis. Data were analyzed using an unpaired two-tailed *t*-test. *P* value of less than 0.05 was considered to be significant.

Results

CXCR4 expression in BMDCs and LCs

Initially, we evaluated the expression levels of CXCR4 on BMDCs by flow cytometry. BM cells were incubated in the culture medium with GM-CSF for 5 days. Significant amounts of CXCR4 were detected in the $CD11c^+$ BMDCs, but $CD11c^-$ fraction expressed CXCR4 to a much lesser degree (Fig. 1A). We then compared the expression level of LCs. Among epidermal cell suspensions, CXCR4 was expressed on MHC class II^+ epidermal LCs but merely barely detected on MHC class II^- KCs (Fig. 1B).

Reduction of BMDC and LC numbers by CXCR4 antagonist treatment

To address whether CXCR4 signaling is involved in the functions of DCs, we added CXCR4 antagonist to BMDC cultures. Two-day treatment with this antagonist significantly decreased the numbers of both mature $CD11c^+$ MHC class II^{high+} DCs and immature $CD11c^+$ MHC class II^{low+} DCs (Fig. 2A and B). Moreover, CXCR4 antagonist suppressed the number of the mature subset of DCs more markedly than that of the immature subset (Fig. 2C). These

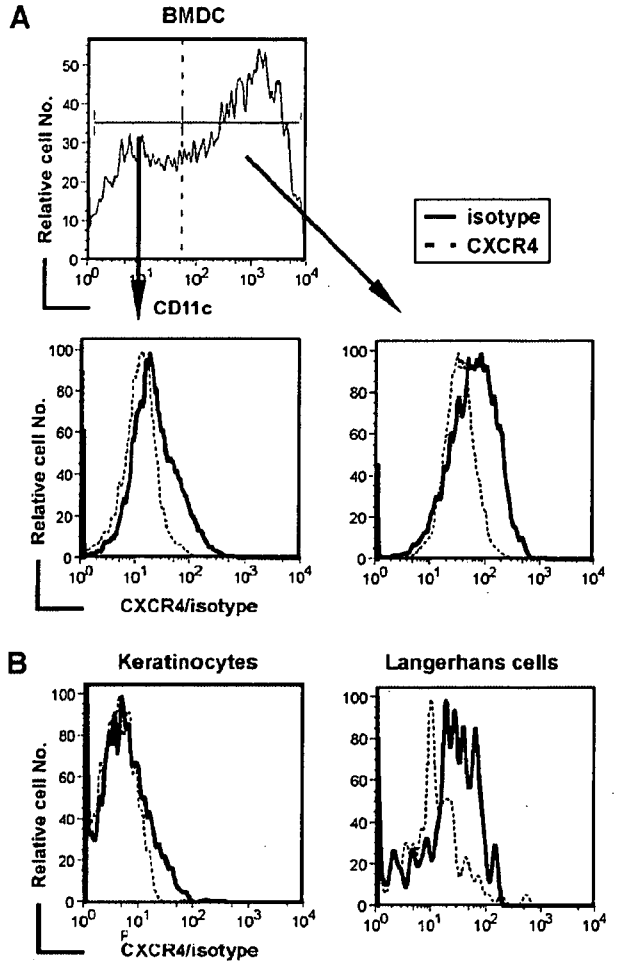

Fig. 1. CXCR4 expression on BMDCs and LCs. (A) BMDCs were prepared after 5 day culture of BM cells with GM-CSF. The expression of CXCR4 on $CD11c^+$ BMDCs and $CD11c^-$ non-DC fraction was evaluated. (B) Epidermal cell suspensions were prepared, and MHC class II^+ LCs and MHC class II^- keratinocytes were evaluated for CXCR4 expression. The profiles show flow cytometric analysis of the cells with the indicated markers, and as a control, rat IgG2a isotype-matched control was used.

results indicated that CXCR4 engagement promoted the maturation, and survival and/or proliferation of DCs. On the other hand, it was reported that CXCR4 is expressed by human cutaneous DCs using immunohistochemical and flow cytometric analyses [15]. We detected a significant amount of CXCL12 in the culture medium (8.8 ± 3.6 ng/ml, $n = 3$) after BMDC incubation.

We then prepared epidermal cell suspensions from mouse earlobes and cultured them for 2 days. CXCR4 antagonist reduced the number of both $CD11c^+$ MHC class II^{high+} mature LCs and $CD11c^+$ MHC class II^{int+} immature LCs (Fig. 3A). It was reported that epidermal LCs are unable to proliferate in vitro when they are incubated as epidermal cell suspension [16]. Our results together with the previous report suggest that CXCR4 signaling promotes the survival of LCs. Moreover, we examined the expression of other co-stimulatory molecules and

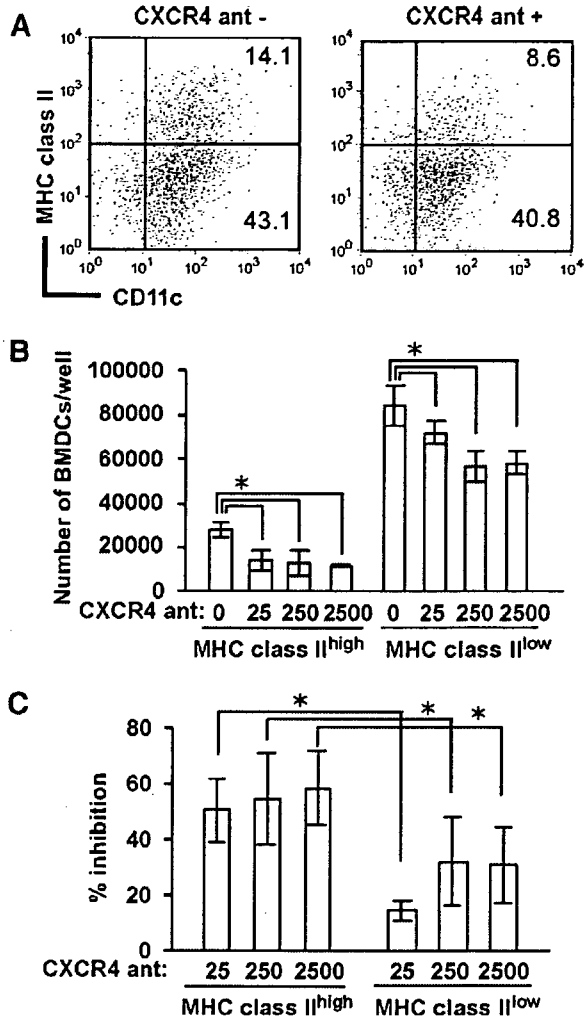

Fig. 2. Reduction of BMDC numbers by CXCR4 antagonist. (A–C) Five day cultured BMDCs were incubated for additional 2 days in the absence (CXCR4 ant−) or presence of CXCR4 antagonist (CXCR4 ant+) at 25, 250, or 2500 ng/ml and analyzed by flow cytometry. The number represents the frequency of each gated group (%) (A). Numbers of $CD11c^+$ MHC class II^{high+} mature BMDCs and $CD11c^+$ MHC class II^{low+} immature BMDCs per well were shown (B). The % inhibition by CXCR4 on each subset was shown (C). Columns show the mean ± SD from triplicated wells. Student's t test was performed between the indicated groups and an asterisk indicates $P < 0.05$. Data are a representative of three independent experiments.

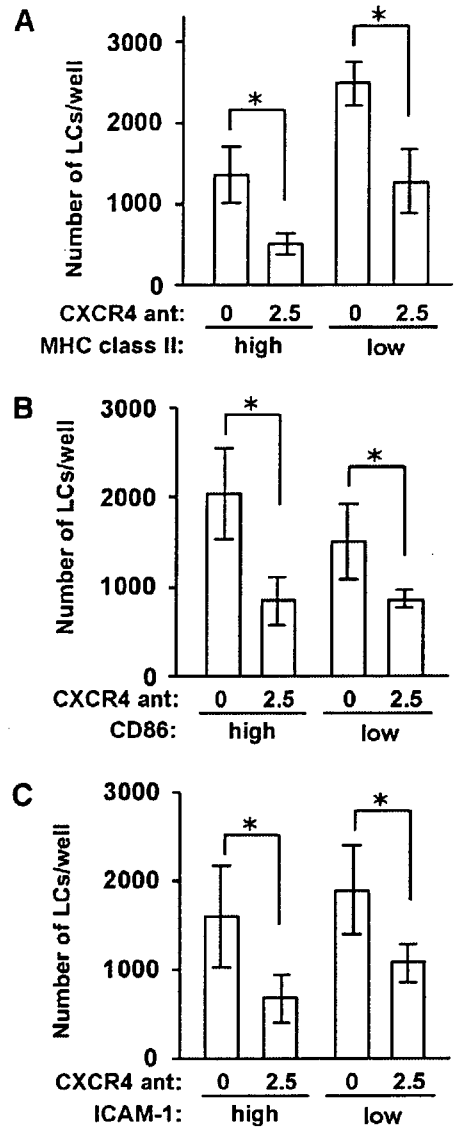

Fig. 3. Reduction of LC numbers by CXCR4 antagonist. Freshly isolated epidermal cell suspensions were incubated for 2 days in the presence or absence of 2.5 μg/ml of CXCR4 antagonist, and the numbers of $CD11c^+$ MHC class II^{high+} and MHC class II^{low+} LC subsets (A), $CD11c^+$ $CD86^{high+}$ and $CD86^{low+}$ LC subsets (B), and $CD11c^+$ $CD54^{high+}$ and $CD54^{low+}$ LC subsets (C) were measured. Columns show the mean ± SD from triplicated wells. Student's t test was performed between the indicated groups and an asterisk indicates $P < 0.05$. Data are a representative of three independent experiments.

adhesion molecules on LCs. CXCR4 antagonist decreased the number of both $CD86^{high+}$ and $CD86^{low+}$ LCs, and $CD54^{high+}$ and $CD54^{low+}$LCs (Fig. 3B and C). The intensity of suppression was more significant in $CD86^{high+}$ and $CD54^{high+}$ LC subsets than in $CD86^{low+}$ and $CD54^{low+}$ LC subsets (Fig. 3B and C). Therefore, CXCR4 antagonist seemed to attenuate LC maturation.

Augmentation of DC-dependent hapten specific T cell proliferation by CXCL12

The relevance of the observed CXCR4-mediated regulation of DC function to immune responses is a matter to be clarified. B6 mice were sensitized with DNFB hapten applied onto the abdomen. Five days later, the regional lymph node cells were isolated, and the responsiveness of primed T cells to DNBS, a water-soluble compound with the same antigenicity as DNFB, was tested in the presence or absence of recombinant murine CXCL12 or CXCR4 antagonist. The proliferative response of lymph node cells was enhanced by CXCL12 and suppressed by CXCR4 antagonist (Fig. 4). Such effects were not observed when 2×10^5 $CD4^+$ cells were stimulated with 10 ng/ml phorbol

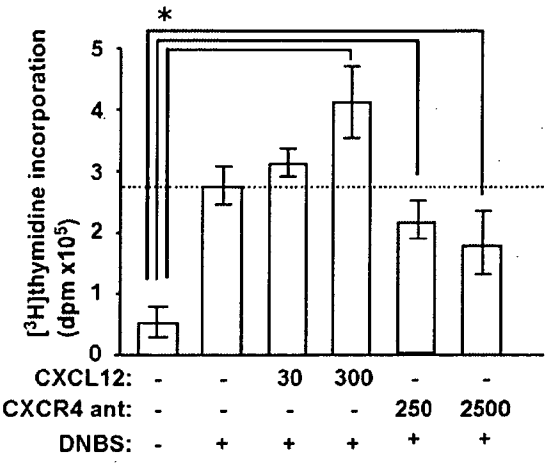

Fig. 4. Modulation of T cell-stimulatory capacity of DCs by CXCL12–CXCR4 engagements. The proliferate response of DNFB-sensitized lymphocytes to DNBS was measured in triplicate with or without CXCL12 at 30 or 300 ng/ml, or CXCR4 antagonist at 250 or 2500 ng/ml. Student's t test was performed an asterisk indicates $P < 0.05$. Results are a representative of three independent experiments. d.p.m; decay per minute.

myristate acetate (Sigma Chemical) and 1 μM ionomycin (Wako, Osaka, Japan), a stimulation procedure independent of DC stimulation (data not shown). This is interpreted as an indication that CXCL12 up-modulates the antigen-presenting ability of DCs for T cells via CXCR4.

Discussion

It is a well accepted concept that chemokines are involved in not only chemotaxis but also other cellular events, such as survival, adhesion, proliferation, and differentiation [3]. For example, the roles of CCR7 on DCs have been well characterized in terms of maturation and differentiation [3]. On the other hand, the roles of CXCR4 on DCs remained largely unknown. Here, we showed that the numbers of BMDCs and LCs were decreased by CXCR4 antagonist in vitro. It is considered that LCs are incapable of proliferating in vitro when cultured as epidermal cell suspensions [16]. These results suggest that CXCR4 promotes DC survival. In fact, it was reported that CXCR4 signaling prolongs BM stromal stem cell and plasma cell survival [17,18]. In addition, CXCR4 antagonist decreased the number of the mature subsets of BMDCs and LCs than those of the immature ones. Consistently, the proliferative response of sensitized lymph node cells by re-stimulation in vitro was enhanced by CXCL12 and suppressed by CXCR4 antagonist. These data suggest that CXCL12–CXCR4 engagement controls DC survival and maturation.

Once foreign antigens are exposed to the skin, LCs and dermal DCs take up antigens and migrate into regional lymph nodes through lymphatic vessels. At present, it is not certain how and where these LCs and dermal DCs meet CXCL12 producing cells. CXCL12 was known to be detected in murine lymphatic vessels by our immunohistochemical analysis [7]. CXCL12 from lymphatic vessels may be important for DC survival and maturation as well as DC chemotaxis. Accordingly, FITC-induced cutaneous DC migration into regional lymph nodes was impaired by CXCR4 antagonist [7]. On the other hand, it was reported that CXCR4 is expressed by human cutaneous DCs using immunohistochemical and flow cytometric analyses [15]. We detected a significant amount of CXCL12 in the culture medium. It is possible that CXCL12 produced by DCs autonomously stimulates DCs themselves through CXCR4 and thus prolongs cell survival.

Our present study suggests that CXCL12–CXCR4 engagement may play an important role for the initiation of acquired skin immune response. Consistently, CXCR4 antagonist reduced mouse hapten-induced contact hypersensitivity response [7]. Because of embryonic lethality of CXCR4 knockout mice [19–21], CXCR4 antagonist can be a useful chemical reagent to evaluate the role of CXCR4 on DCs. Understanding of factors that determine cutaneous DC functions might offer new opportunities for therapeutic intervention to suppress or stimulate the immune response.

Acknowledgments

We thank Ms. Junko Nagai for technical assistance. The authors have no conflicting financial interests. This work was supported in part by grants from the Ministry of Education, Culture, Sports, Science, and Technology of Japan, Takeda Research Foundation, Cosmetology Research Foundation, Ono Research Foundation, and Lydia O'Leary Memorial Foundation.

References

[1] J. Banchereau, R.M. Steinman, Dendritic cells and the control of immunity, Nature 392 (1998) 245–252.
[2] G.J. Randolph, V. Angeli, M.A. Swartz, Dendritic-cell trafficking to lymph nodes through lymphatic vessels, Nat. Rev. Immunol. 5 (2005) 617–628.
[3] N. Sanchez-Sanchez, L. Riol-Blanco, J.L. Rodriguez-Fernandez, The multiple personalities of the chemokine receptor CCR7 in dendritic cells, J. Immunol. 176 (2006) 5153–5159.
[4] F. Sallusto, P. Schaerli, P. Loetscher, C. Schaniel, D. Lenig, C.R. Mackay, S. Qin, A. Lanzavecchia, Rapid and coordinated switch in chemokine receptor expression during dendritic cell maturation, Eur. J. Immunol. 28 (1998) 2760–2769.
[5] H. Saeki, A.M. Moore, M.J. Brown, S.T. Hwang, Cutting edge: secondary lymphoid-tissue chemokine (SLC) and CC chemokine receptor 7 (CCR7) participate in the emigration pathway of mature dendritic cells from the skin to regional lymph nodes, J. Immunol. 162 (1999) 2472–2475.
[6] J.Y. Humrich, J.H. Humrich, M. Averbeck, P. Thumann, C. Termeer, E. Kampgen, G. Schuler, L. Jenne, Mature monocyte-derived dendritic cells respond more strongly to CCL19 than to CXCL12: consequences for directional migration, Immunology 117 (2006) 238–247.
[7] K. Kabashima, N. Shiraishi, K. Sugita, T. Mori, A. Onoue, M. Kobayashi, J. Sakabe, R. Yoshiki, H. Tamamura, N. Fujii, K. Inaba, Y. Tokura, CXCL12–CXCR4 engagement is required for migration of cutaneous dendritic cells, Am. J. Pathol., in press.

[8] H. Tamamura, K. Hiramatsu, M. Mizumoto, S. Ueda, S. Kusano, S. Terakubo, M. Akamatsu, N. Yamamoto, J.O. Trent, Z. Wang, S.C. Peiper, H. Nakashima, A. Otaka, N. Fujii, Enhancement of the T140-based pharmacophores leads to the development of more potent and bio-stable CXCR4 antagonists, Org. Biomol. Chem. 1 (2003) 3663–3669.

[9] H. Tamamura, A. Hori, N. Kanzaki, K. Hiramatsu, M. Mizumoto, H. Nakashima, N. Yamamoto, A. Otaka, N. Fujii, T140 analogs as CXCR4 antagonists identified as anti-metastatic agents in the treatment of breast cancer, FEBS Lett. 550 (2003) 79–83.

[10] A.C. Zannettino, A.N. Farrugia, A. Kortesidis, J. Manavis, L.B. To, S.K. Martin, P. Diamond, H. Tamamura, T. Lapidot, N. Fujii, S. Gronthos, Elevated serum levels of stromal-derived factor-1alpha are associated with increased osteoclast activity and osteolytic bone disease in multiple myeloma patients, Cancer Res. 65 (2005) 1700–1709.

[11] K. Inaba, M. Inaba, N. Romani, H. Aya, M. Deguchi, S. Ikehara, S. Muramatsu, R.M. Steinman, Generation of large numbers of dendritic cells from mouse bone marrow cultures supplemented with granulocyte/macrophage colony-stimulating factor, J. Exp. Med. 176 (1992) 1693–1702.

[12] Y. Tokura, J. Yagi, M. O'Malley, J.M. Lewis, M. Takigawa, R.L. Edelson, R.E. Tigelaar, Superantigenic staphylococcal exotoxins induce T-cell proliferation in the presence of Langerhans cells or class II-bearing keratinocytes and stimulate keratinocytes to produce T-cell-activating cytokines, J. Invest. Dermatol. 102 (1994) 31–38.

[13] A. Kocikova, A. Kolesaric, F. Koszik, G. Stingl, A. Elbe-Burger, Murine Langerhans cells cultured under serum-free conditions mature into potent stimulators of primary immune responses in vitro and in vivo, J. Immunol. 161 (1998) 4033–4041.

[14] K. Kabashima, N.M. Haynes, Y. Xu, S.L. Nutt, M.L. Allende, R.L. Proia, J.G. Cyster, Plasma cell S1P1 expression determines secondary lymphoid organ retention versus bone marrow tropism, J. Exp. Med. 203 (2006) 2683–2690.

[15] J.L. Pablos, A. Amara, A. Bouloc, B. Santiago, A. Caruz, M. Galindo, T. Delaunay, J.L. Virelizier, F. Arenzana-Seisdedos, Stromal-cell derived factor is expressed by dendritic cells and endothelium in human skin, Am. J. Pathol. 155 (1999) 1577–1586.

[16] G. Schuler, R.M. Steinman, Murine epidermal Langerhans cells mature into potent immunostimulatory dendritic cells in vitro, J. Exp. Med. 161 (1985) 526–546.

[17] A. Kortesidis, A. Zannettino, S. Isenmann, S. Shi, T. Lapidot, S. Gronthos, Stromal-derived factor-1 promotes the growth, survival, and development of human bone marrow stromal stem cells, Blood 105 (2005) 3793–3801.

[18] K. Tokoyoda, T. Egawa, T. Sugiyama, B.I. Choi, T. Nagasawa, Cellular niches controlling B lymphocyte behavior within bone marrow during development, Immunity 20 (2004) 707–718.

[19] T. Nagasawa, S. Hirota, K. Tachibana, N. Takakura, S. Nishikawa, Y. Kitamura, N. Yoshida, H. Kikutani, T. Kishimoto, Defects of B-cell lymphopoiesis and bone-marrow myelopoiesis in mice lacking the CXC chemokine PBSF/SDF-1, Nature 382 (1996) 635–638.

[20] Y.R. Zou, A.H. Kottmann, M. Kuroda, I. Taniuchi, D.R. Littman, Function of the chemokine receptor CXCR4 in haematopoiesis and in cerebellar development, Nature 393 (1998) 595–599.

[21] Q. Ma, D. Jones, P.R. Borghesani, R.A. Segal, T. Nagasawa, T. Kishimoto, R.T. Bronson, T.A. Springer, Impaired B-lymphopoiesis, myelopoiesis, and derailed cerebellar neuron migration in CXCR4- and SDF-1-deficient mice, Proc. Natl. Acad. Sci. USA 95 (1998) 9448–9453.

Development of Low Molecular Weight CXCR4 Antagonists by Exploratory Structural Tuning of Cyclic Tetra- and Pentapeptide-Scaffolds Towards the Treatment of HIV Infection, Cancer Metastasis and Rheumatoid Arthritis

Hirokazu Tamamura*,[1], Hiroshi Tsutsumi[1], Hiroyuki Masuno[1] and Nobutaka Fujii*,[2]

[1]*Institute of Biomaterials and Bioengineering, Tokyo Medical and Dental University, Chiyoda-ku, Tokyo 101-0062, Japan*

[2]*Graduate School of Pharmaceutical Sciences, Kyoto University, Sakyo-ku, Kyoto 606-8501, Japan*

Abstract: The chemokine receptor, CXCR4, is a GPCR that transduces signals of its endogenous ligand, CXCL12 (stromal cell-derived factor-1, SDF-1). The CXCL12-CXCR4 system plays an important role in the migration of progenitors during embryologic development of the cardiovascular, hemopoietic, central nervous systems, etc. This system has recently been proven to be involved in several problematic diseases, including HIV infection, cancer cell metastasis, leukemia cell progression, rheumatoid arthritis (RA) and pulmonary fibrosis. Thus, CXCR4 is thought to be an important therapeutic target to overcome the above diseases. Fourteen-mer peptides, T140 and its analogs, were previously found to be specific CXCR4 antagonists that were characterized as HIV-entry inhibitors, anti-cancer-metastatic agents, anti-chronic lymphocytic/acute lymphoblastic leukemia agents and anti-RA agents. Based on our knowledge of pharmacophores of T140, CXCR4 antagonists, such as FC131, were previously found by the efficient utilization of cyclic pentapeptide libraries. This review article focuses on our recent research on the development of low molecular weight CXCR4 antagonists including FC131 analogs, in which structural tuning of the cyclic peptide ring and chemical modifications were performed for an increase in potency and a reduction of the peptide character.

Keywords: Leukemia cell progression, cancer metastasis, chemokine receptor, HIV infection, low molecular weight CXCR4 antagonist, rheumatoid arthritis, chemical biology, proteomics.

INTRODUCTION

Since elucidation of human genome, proteomics has been prosperous in biology and life science. In a postgenome era, artificial functional molecules involving selective agonists and antagonists are highly useful for studies of chemical biology. Seven transmembrane (7TM) G-protein-coupled receptor (GPCR) families are important targets in proteomics, and thus, specific probes for GPCRs can accelerate studies of proteomics and chemical biology [1]. Chemokine receptors are classified into GPCR families, which transduce signals of the corresponding chemokines. Chemokines and their receptors play fundamental roles in physiological phenomena. Chemokines belong to a chemotactic cytokine family that attracts and induces migration of leukocytes. The relationships between chemokines and their receptors are highly inter-connected and complicated: a single chemokine recognizes a plurality of receptors, while one chemokine receptor recognizes several chemokines. Numerous chemokines lack receptor selectivity. However, the chemokine receptor CXCR4 possesses the chemokine, CXCL12/stromal cell-derived factor-1 (SDF-1) as its solitary ligand [2-5]. The CXCL12-CXCR4 axis plays a fundamental role in the migration of progenitor cells during embryonic development of the cardiovascular, intestine vascular [6], hemopoietic [7], central nervous [8] systems and so on. However, its physiological roles in adults remain poorly disclosed. This axis has also been shown to be involved in several problematic diseases such as HIV infection [9], cancer cell metastasis [10-27], leukemia cell progression [28-30], rheumatoid arthritis (RA) [31] and pulmonary fibrosis [32] (Fig. (1)). First, CXCR4 was identified as the second cellular receptor following CD4 for the T cell line-tropic (X4-) HIV-1 entry [9]. X4 HIV-1 strains constitute majority in the late stage of HIV infection and AIDS, while macrophage-tropic (R5-) HIV-1 strains, which utilize the chemokine receptor CCR5 as another second receptor, do in the early stage of HIV infection [33-37]. Recently, a dynamic supramolecular mechanism in the HIV entry/fusion process during the HIV-1 replication has been elucidated in detail: At first, an envelope protein gp120 binds to a cell surface protein CD4 followed by a conformational change of gp120 and its subsequent binding to the above second receptor, CCR5 or CXCR4. The binding leads to penetration of an another envelope protein, gp41, anchoring HIV envelope into membrane, to the cell membrane from the *N*-terminus end followed by subsequent formation of the gp41 trimer-of-hairpins structure in the center region, which causes membrane fusion of HIV/cells and finally results in completion of the infection [38]. Since elucidation of the above dynamic molecular machinery, the development of effective inhibitors blocking HIV-entry/fusion has been expected. Second, lots of papers have reported that several types of cancers overexpress CXCR4 on the surface of cells, and that CXCL12 is highly expressed in

*Address correspondence to these authors at the [1]Institute of Biomaterials and Bioengineering, Tokyo Medical and Dental University, Chiyoda-ku, Tokyo 101-0062, Japan; Tel: +81-3-5280-8036; Fax: +81-3-5280-8039; E-mail: tamamura.mr@tmd.ac.jp

[2]Graduate School of Pharmaceutical Sciences, Kyoto University, Sakyo-ku, Kyoto 606-8501, Japan; Tel: +81 75 753 4551, Fax: +81 75 753 4570; E-mail: nfujii@pharm.kyoto-u.ac.jp

0929-8673/07 $50.00+.00